



Contents lists available at ScienceDirect

Plant Physiology and Biochemistry

journal homepage: www.elsevier.com/locate/plaphy

Abscisic acid, stress and ripening (ASR) proteins play a role in iron homeostasis in rice (*Oryza sativa* L.)

Lucas Roani Ponte^a , Jover da Silva Alves^a , Yugo Lima-Melo^a, Paloma Koprovski Menguer^a, Hadrien Georges Boulanger^b, Ricardo Fabiano Hettwer Giehl^c, Cristiane Paula Gomes Calixto^b, Márcia Margis-Pinheiro^{a,d} , Felipe Klein Ricachenevsky^{a,e,*} 

^a Programa de Pós-Graduação em Biologia Celular e Molecular (PPGBCM), Centro de Biotecnologia, Universidade Federal do Rio Grande do Sul, Porto Alegre, RS, Brazil

^b Departamento de Botânica, Instituto de Biociências, Universidade de São Paulo, São Paulo, Brazil

^c Leibniz Institute of Plant Genetics and Crop Plant Research (IPK) OT Gatersleben, Seeland, Germany

^d Departamento de Genética, Universidade Federal do Rio Grande do Sul, Porto Alegre, Brazil

^e Departamento de Botânica, Universidade Federal do Rio Grande do Sul, Porto Alegre, Brazil

ARTICLE INFO

Keywords:

Iron
Abscisic acid/stress/ripening
Chlorosis
Rice
Ionome

ABSTRACT

Iron (Fe) is essential for plant growth, playing a key role in photosynthesis, respiration, and nitrogen fixation. Despite its abundance, Fe is not easily available for uptake by roots, making Fe deficiency a common issue that reduces crop yields. The ASR (Abscisic acid/Stress/Ripening) proteins are known to be responsive to different abiotic stresses. Two ASR proteins from rice (*Oryza sativa* L.), OsASR1 and OsASR5, were described as transcription factors involved in aluminum (Al) toxicity response, and were shown to be partially redundant in their function. Here we explored a possible role of ASR proteins in Fe deficiency in rice plants. We showed that rice plants silenced for ASR genes (named OsASR5-RNAi) had increased sensitivity to Fe deficiency, with early and more severe chlorosis, as well as reduced photosynthesis, stunted growth, reduced seed set and altered ionome in roots, leaves and seeds. Transcriptomic analysis indicated that roots of OsASR5-RNAi plants had similar expression of Fe uptake genes, such as *OsIRT1* and *OsYSL15*. However, long distance phloem transporter *OsYSL2* was up-regulated in OsASR5-RNAi roots to a larger extent compared to WT, suggesting ASR proteins negatively regulate *OsYSL2* expression. We also identified other interesting candidate genes, such as *OsZIFL2* and *Thionins*, that are dependent on ASR proteins for regulation under Fe deficiency. Our work demonstrated that OsASR proteins are important for proper Fe deficiency response in rice.

1. Introduction

Iron (Fe) is essential for plants. It is present in the structure of several proteins and complexes that participate in electron transfer reactions during photosynthesis and respiration, including photosystems I and II, ferredoxins and cytochromes (Przybyla-Toscano et al., 2021). Fe is also a critical cofactor for nitrogenase used in symbiotic nitrogen fixation by rhizobia (Liu et al., 2023; Sankari et al., 2022). However, despite being abundant in the Earth's lithosphere, Fe is not readily available for uptake by plant roots. Consequently, crops tend to be susceptible to Fe deficiency (Trofimov et al., 2024). Often manifested as leaf chlorosis, Fe deficiency impairs photosynthesis, resulting in stunted growth, delayed

flowering and yield losses (Huang and Suen, 2021; Krohling et al., 2016). On other hand, Fe excess can be harmful, since Fe can produce reactive oxygen species (ROS) by Fenton's reactions, leading to toxicity (Becana et al., 1998; Wairich et al., 2024). Therefore, Fe homeostasis must be finely regulated to ensure adequate Fe concentrations in different plant tissues.

Plants have two strategies for Fe uptake, known as Strategy I and Strategy II (Rodrigues et al., 2023; Wairich et al., 2022). Strategy I is performed by non-grass plants and is based on the solubilization of ferric ion (Fe^{3+}) by the release of H^+ protons into the rhizosphere; reduction of Fe^{3+} to ferrous ion (Fe^{2+}) by ferric chelate reductases, such as FRO2 (Robinson et al., 1999; Connolly et al., 2003); and Fe^{2+} uptake by high

This article is part of a special issue entitled: Plant stress responses published in Plant Physiology and Biochemistry.

* Corresponding author. Programa de Pós-Graduação em Biologia Celular e Molecular (PPGBCM), Centro de Biotecnologia, Universidade Federal do Rio Grande do Sul, Porto Alegre, RS, Brazil.

E-mail address: felipecruzalta@gmail.com (F.K. Ricachenevsky).

<https://doi.org/10.1016/j.plaphy.2025.109882>

Received 16 January 2025; Received in revised form 29 March 2025; Accepted 2 April 2025

Available online 2 April 2025

0981-9428/© 2025 Elsevier Masson SAS. All rights are reserved, including those for text and data mining, AI training, and similar technologies.

affinity plasma membrane transporters, such as IRT1 (Iron-Regulated Transporter 1) (Eide et al., 1996; Korshunova et al., 1999; Vert et al., 2002). On the other hand, Strategy II is performed by grasses and is based on the release of Fe^{3+} chelators, named phytosiderophores (PSs), into the rhizosphere (Carrillo and Borthakur, 2021; Nozoye et al., 2011). The intact Fe^{3+} -PS complexes are then taken up by YS1/YSL15 (Yellow-Stripe Like) transporters (Curie et al., 2001; Inoue et al., 2009; Lee et al., 2009). Plants within the *Oryza* genus, including rice (*Oryza sativa* L.), use the Combined Strategy, which consists of Strategy II coupled with the up-regulation of an IRT-like transporter, allowing these species to uptake both Fe^{3+} -PS complexes and Fe^{2+} ions (Ishimaru et al., 2006; Wairich et al., 2019).

Aluminum (Al^{3+}) toxicity is another common disorder for plants, resulting in significant yield losses. Al toxicity is typically observed in acidic soils, particularly in pH lower than 5.5. Under these conditions, Al is highly soluble and readily available for uptake by roots (Bojórquez-Quintal et al., 2017). Because of that, plants have developed mechanisms to tolerate Al toxicity. Al-tolerant plant species are known to release organic acids into the rhizosphere, such as citrate, malate and oxalate, which chelate Al^{3+} ions and prevent their entry into roots (Yang et al., 2019). In parallel, to minimize Al toxic effects on vital cellular processes, some Al-tolerant plants also show enhanced antioxidant defense systems, including the production of enzymes, such as superoxide dismutase, catalase, and peroxidases, to scavenge ROS (Ranjan et al., 2021). Furthermore, uptake by plasma membrane and subsequent vacuolar detoxification of Al^{3+} in root and/or shoot cells is also described (Yan et al., 2022).

Rice has been used as a model plant for studying Fe homeostasis due to its genetic and physiological similarities with other important cereal crops such as bread wheat (*Triticum aestivum* L.), barley (*Hordeum vulgare* L.) and maize (*Zea mays* L.) (Kim et al., 2014; Song et al., 2018). The presence of the combined strategy in rice allows comparisons with Strategy I plants, with several homologous proteins playing similar roles in upstream regulatory networks and uptake mechanisms (Grillet and Schmidt, 2019; Wairich et al., 2025), as well as with Strategy II plants, for which rice is a good model given its small genome and availability of tools for molecular genetics. Since rice is usually cultivated in acidic soils, it provides an ideal system to investigate the adaptive responses and tolerance mechanisms of plants under Al toxicity (Arenhart et al., 2015; Zhang et al., 2019). Moreover, rice is considered the most Al-tolerant cereal (Famoso et al., 2010). Interestingly, Al has been shown to affect Fe homeostasis in rice as the supply of Al alleviated the chlorotic phenotype of Fe-deficient plants (Alves et al., 2025). It was suggested that Al could be causing P deficiency, which is known to alleviate Fe deficiency-induced chlorosis (Nam et al. 2021; Therby-Vale et al., 2022). However, little is known about the underlying mechanisms, and which proteins could be involved in regulating both Al toxicity and Fe deficiency responses.

The *ASR* (*Abscisic acid/Stress/Ripening*) genes are plant-specific proteins known to be involved in fruit ripening, sugar metabolism and to be responsive to different abiotic stresses, such as drought, salinity and cold (Jia et al., 2016; Li et al., 2018; Parrilla et al., 2022; Yacoubi et al., 2022). There are six *ASR* genes in the rice genome, and since *ASR* genes are not present in the *Brassicaceae* family, rice is the model of choice to understand the function of these proteins in plants (Parrilla et al., 2022; Philippe et al., 2010). Two members of the *OsASR* family, namely *OsASR1* and *OsASR5*, were linked to Al stress response in rice (Arenhart et al., 2013, 2014, 2016). Both genes are responsive to Al stress (Arenhart et al., 2013). *OsASR5* was shown to control several Al-responsive genes by directly binding to their promoters (Arenhart et al., 2014). It was shown that *OsASR1* and *OsASR5* can functionally compensate for each other at Al responsive target gene promoters, suggesting that these genes have at least partial functional redundancy (Arenhart et al., 2016). Among other Al-responsive genes, *OsASR5* is able to directly bind to *Sensitive To Al Rhizotoxicity 1* (*OsSTAR1*) promoter and is involved in *OsSTAR1* up-regulation in Al toxicity (Arenhart

et al., 2014; Huang et al., 2009). *OsSTAR1* is also named *Efflux transporter of NA 2* (*OsENA2*), which has a role in Fe homeostasis (Nozoye et al., 2011). Moreover, *OsASR* transcripts have been found to be responsive to Fe in transcriptomic studies (Stein et al., 2019; Wairich et al., 2019, 2021). However, whether these proteins play a role in Fe homeostasis has hitherto remained unexplored.

Here we evaluated how knockdown rice plants of *ASR* genes respond to Fe deficiency. We found that down-regulation of the *OsASR* genes increases sensitivity to low Fe, with early onset and more pronounced leaf chlorosis, and decreases photosynthesis, growth and seed set. We also found that the mineral element composition of seeds, root and leaf tissues are altered. Transcriptomic analyses in roots indicate that *OsASR5*-RNAi phenotype is not associated with the main Fe deficiency pathway, i.e., regulating *OsYSL15* and *OsIRT1* transporters. However, *OsYSL2* is strongly up-regulated in *OsASR5*-RNAi plants, suggesting that Fe distribution might be involved in the observed phenotype. Our work demonstrates that *ASR* proteins play a role in Fe homeostasis.

2. Material and methods

2.1. Plant materials and growth

We used *Oryza sativa* L. cv Nipponbare and the previously described *OsASR5*-RNAi line (Arenhart et al., 2013). *OsASR5*-RNAi line have been characterized in detail in several other papers of our group (Arenhart et al., 2013, 2014, 2016). The construct decreases expression of several *OsASR* transcripts (see data below; Fig. 8).

Seeds of both genotypes were germinated in Petri dishes with filter paper and distilled water for 7 days and transferred to vermiculite. After two weeks, plants were transferred to a hydroponic system. The nutrient solution consisted of 700 μM K_2SO_4 , 100 μM KCl , 100 μM KH_2PO_4 , 2 mM $\text{Ca}(\text{NO}_3)_2$, 500 μM MgSO_4 , 10 μM H_3BO_3 , 0.5 μM MnSO_4 , 0.5 μM ZnSO_4 , 0.2 μM CuSO_4 , 0.01 μM $(\text{NH}_4)_6\text{Mo}_7\text{O}_{24}$, and 100 μM Fe^{3+} -EDTA. The pH of the nutrient solution was adjusted to 5.4 and the solution was renewed twice a week. Plants were exposed to treatments after two weeks of acclimation. For Fe deficiency treatment (-Fe), Fe was omitted from nutrient solution, while control plants were cultivated in complete nutrient solution. Plants were kept under treatment or under control condition (CC) for up to 24 days. Growth conditions were $27^\circ\text{C} \pm 1^\circ\text{C}$ under photoperiod of 16h/8h light/dark and irradiance of 150 $\mu\text{mol photons m}^{-2} \text{s}^{-1}$. Plants grown until maturity were cultivated in greenroom conditions with photoperiod of 12h/12h light/dark and irradiance of 200 $\mu\text{mol photons m}^{-2} \text{s}^{-1}$.

2.2. Growth measurements and agronomic traits

Measurements of shoot height and root length of individual plants ($n = 5$) were performed using a graduated ruler. Shoot and root samples were dried in a forced ventilation oven at 60°C for one week. The dry mass values were obtained using an analytical precision balance. At maturity, plants were evaluated for total number of panicles and number of filled and empty seeds ($n = 12$ to 24).

2.3. SPAD, gas exchange and fluorescence analyses

The relative chlorophyll content were measured with the Soil Plant Analysis Development (SPAD) chlorophyll meter SPAD 502 (Konica Minolta, Inc., Tokyo, Japan) from the 11th to the 21st day of treatment every two days. Measurements were performed in the central region of the fifth fully expanded leaf of the same plant. Data was obtained from five different plants ($n = 5$).

Gas exchange and chlorophyll *a* fluorescence was measured in the youngest fully expanded leaves from both WT and *OsASR5*-RNAi lines under control condition or -Fe. The measurements were performed at the 7th, 14th, and 21st days of treatment. CO_2 assimilation rate (A ; $\mu\text{mol CO}_2 \text{ m}^{-2} \text{ s}^{-1}$), stomatal conductance (g_s ; $\text{mol H}_2\text{O m}^{-2} \text{ s}^{-1}$), internal CO_2

concentration (C_i ; $\mu\text{mol CO}_2 \text{ mol air}^{-1}$) and transpiration (E ; $\text{mmol H}_2\text{O m}^{-2} \text{ s}^{-1}$) were measured with a LCpro-SD portable InfraRed Gas Analyzer system (IRGA; ADC Bioscientific, Hoddesdon, England). The internal parameters in the IRGA chamber during gas exchange measurements were: 27 °C, 1000 $\mu\text{mol photons m}^{-2} \text{ s}^{-1}$, 420 ppm CO_2 concentration, ambient humidity ($80 \pm 5 \%$). Each sample corresponded to the normalized value of two leaves from different plants and the measurement recordings were performed 15 min after placing the samples inside the measuring chamber with the internal parameters described previously. The water use efficiency ($\mu\text{mol CO}_2 \text{ mmol H}_2\text{O}^{-1}$) was calculated as A/E and the carboxylation efficiency was calculated as A/C_i . Normalized data is used for figures presentation.

In vivo chlorophyll *a* fluorescence was measured using an OS-30p chlorophyll fluorometer (Opti-Sciences, Hudson, NH, USA). The fluorescence parameters were measured by the saturation pulse method (Schreiber et al., 1995). The maximum and the minimum fluorescence (F_m and F_o , respectively) were measured in 30-min dark-adapted plants and the maximum quantum yield of photosystem II (PSII) [F_v/F_m ; ($F_m - F_o$)/ F_m] was calculated.

2.4. Mineral element analyses

Whole root or leaf samples were dried at 65 °C and weighed in polytetrafluoroethylene tubes. Samples were digested with concentrated HNO_3 (67–69 %; Bernd Kraft) and pressurized in a high-performance microwave reactor (UltraCLAVE IV, MLS GmbH). The digested samples were diluted with deionized water (Milli-Q Reference A+, Merck Millipore). Elemental analysis was carried out by high resolution inductively coupled plasma mass spectrometry (HR-ICP-MS) (ELEMENT 2, Thermo Fisher Scientific, Germany).

Elemental concentration of seeds was determined using an inductively couple plasma mass spectrometer (ICP-MS; Elan DRcE, PerkinElmer; or NexION 300D, PerkinElmer) as described previously (Zhang et al., 2014). The radar charts were plotted using the online tool available at <https://www.bioinformatics.com.cn/en> (Tang et al., 2023).

2.5. RNA extraction, library preparation and RNA-seq analyses

For the RNA-seq analyses, plants were cultivated as described above, and roots from 4 plants per sample were collected after five days of treatment. RNA extraction was performed with the Direct-zol™ RNA MiniPrep Plus Kit (Zymo Research). For each treatment and genotype, three libraries ($n = 3$) were sequenced using the Illumina® Nova-Seq6000 system, generating 100 bp paired-end reads.

Pre-processing and analysis of RNA-seq datasets were carried out according to Vitoriano and Calixto (2021). Briefly, residual adaptor sequences were removed from raw paired-end reads using Trimmomatic version 0.39 (Bolger et al., 2014). To generate quantitative transcript-specific expression data, the trimmed reads were pseudo-aligned to the rice reference transcriptome (all cDNAs) available at the MSU Rice Genome Annotation Project Database, Osa1 Release 7 (Kawahara et al., 2013) using Salmon version 1.4.0 (Patro et al., 2017). Full differential gene expression and differential alternative splicing analysis were carried out with the 3D RNA-seq app (Guo et al., 2021).

For this, we firstly generated read counts and Transcript per Million reads (TPM) information from each Salmon output file using tximport R package version 1.10.0 and the lengthScaledTPM method. Next, transcripts with less than 1 count per million (CPM) in ≥ 11 out of 12 samples were removed. Subsequently, the normalization of read counts was carried out across the samples using the weighted Trimmed Mean of M-values (TMM) method. Lastly, the voomWeights pipeline of limma R package was used for differential expression analysis, setting the following thresholds: absolute \log_2 -fold change (L2FC) ≥ 1 and adjusted *P*-value (FDR) ≤ 0.01 . In these analyses, the contrast groups were set as OsASR5-RNAi CC x WT CC, WT –Fe x WT CC, OsASR5-RNAi –Fe x OsASR5-RNAi CC, and OsASR5-RNAi –Fe x WT –Fe, in which “CC”

means control condition and “–Fe” as the Fe deficiency treatment. Raw data can be found at Sequence Read Archive (SRA) database at NCBI (National Center for Biotechnology Information), accession number PRJNA1210584.

Hierarchical clustering was used to partition the differentially expressed genes (DEGs) into 10 clusters with euclidean distance and ward.D clustering algorithm (Saraçlı et al., 2013). ComplexHeatmap R package version 2.16.0 was used to make the heatmap (Gu, 2022).

For the gene ontology (GO) analysis, DEGs were separated into up- and down-regulated genes, taking into account the Fe deficiency treatment in the same genotype [i.e. WT (–Fe x CC) and OsASR5-RNAi (–Fe x CC)]. To identify enriched gene ontologies (Fisher’s test, $P \leq 0.05$), we used the web-based platform Comprehensive Annotation of Rice Multi-Omics (CARMO) (Wang et al., 2015). The Venn diagrams and GO enrichment bubble graphics were plotted using the online tool available at <https://www.bioinformatics.com.cn/en> (Tang et al., 2023).

2.6. Statistical analyses

Our data were tested for normality and homogeneity of variance using the Shapiro-Wilk test and Levene test, respectively. Afterwards, we used Student’s *t*-test or One-Way ANOVA, followed by Tukey’s test, if both assumptions were met. If the data were not normal, we followed with the Mann-Whitney *U* test (for independent samples) or the Kruskal-Wallis test, followed by Dunn’s test for pairwise comparisons (for multiple comparisons). If the data were normal but did not meet the assumption of homogeneity of variance, we performed Welch’s ANOVA, followed by the Games-Howell post-hoc test.

3. Results

3.1. Plants silenced for ASR genes are more sensitive to Fe deficiency

Transgenic rice plants expressing a construct to silence OsASR5 (hereafter OsASR5-RNAi) were previously generated in *Oryza sativa* cv. Nipponbare (hereafter WT) background. The data presented in the original paper and here (see below) show that the expressed construct leads to knockdown of ASR proteins (Arenhart et al., 2013; see below). Since these genes can substitute one another at the promoter binding sites of their target genes and compensate for each other’s loss of function (Arenhart et al., 2016), this transgenic line is excellent for exploring the role of ASR proteins in rice mineral nutrition.

We exposed 30-day-old plants of WT and OsASR5-RNAi genotypes to either control (CC) or Fe deficiency (–Fe) treatments for up to 21 days. Fe deficiency-induced chlorosis was observed in leaves of WT plants but was clearly more pronounced in OsASR5-RNAi (Fig. 1A). To better quantify the differences in Fe deficiency-induced changes in leaf color in WT and OsASR5-RNAi plants, we used SPAD to measure chlorosis in the fifth leaf of both genotypes in a time-course –Fe experiment (Fig. 1B). Measurements started after 11 days after the onset of treatment, since the fifth leaf was the last to fully expand during treatment in both genotypes. While SPAD values were slightly lower in OsASR5-RNAi plants under control condition compared to WT, OsASR5-RNAi plants showed considerably lower values compared to WT control under Fe deficiency plants (Fig. 1B). These data further demonstrate that the knockdown of the OsASR genes lead to more pronounced leaf chlorosis under –Fe.

We also measured shoot height, root length and their respective dry masses of WT and OsASR5-RNAi plants under control condition and –Fe. The shoot height from the two genotypes were similar in control condition, while both shoot height and shoot dry mass were lower in OsASR5-RNAi under –Fe (Fig. 1C and D). While the WT roots were shorter in –Fe than in control, OsASR5-RNAi had roots longer than WT regardless of treatment (Fig. 1E and G). Despite longer roots, OsASR5-RNAi plants showed lower root dry mass compared to WT under –Fe, while being similar in control condition (Fig. 1F and G), suggesting that OsASR5-RNAi plants partition less carbon to roots. Taken together, these

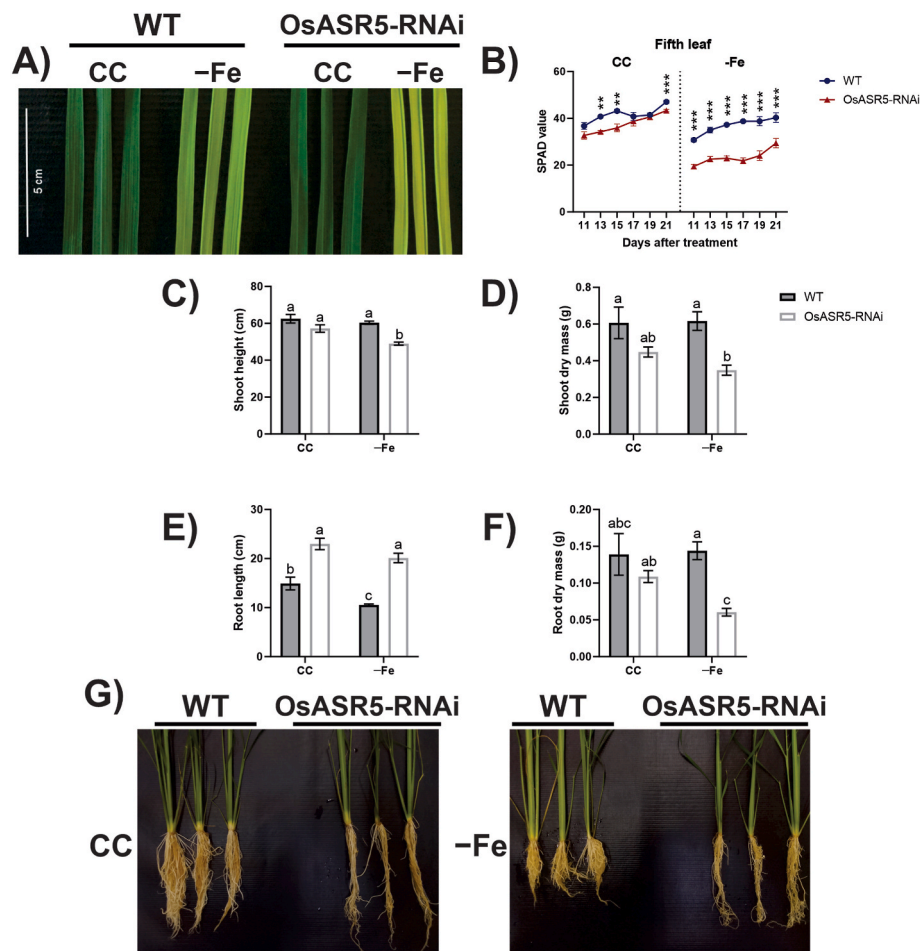


Fig. 1. The phenotype of OsASR5-RNAi plants under Fe deficiency treatment (-Fe). (A) Representative photograph of the fifth leaf of WT and OsASR5-RNAi plants after 21 days of treatment. (B) SPAD values on the fifth leaf of both genotypes during the treatment period. The asterisks denote statistically significant differences between the two genotypes within the same treatment. (C) Shoot height, (D) shoot dry mass, (E) root length and (F) root dry mass of WT and OsASR5-RNAi plants after 23 days of treatment. (G) Representative photographs of the root systems of WT and OsASR5-RNAi plants after 21 days of treatment. Error bars indicate standard error. Statistically significant differences are denoted by asterisks ($*P \leq 0.05$; $**P \leq 0.01$; $***P \leq 0.001$) or by distinct letters. CC = control condition.

results suggest that OsASR5-RNAi plants are more sensitive to -Fe, showing earlier chlorosis and decreased shoot and root biomass accumulation when Fe is low.

3.2. OsASR5-RNAi plants photosynthesis is reduced under Fe deficiency

To quantify possible differences in photosynthesis associated with increased chlorosis in OsASR5-RNAi under -Fe, we quantified photosynthetic parameters at 7, 14 and 21 days of treatment (Fig. 2). -Fe clearly decreased the CO₂ assimilation rate in WT plants at 7 and 21 days, and in OsASR5-RNAi plants at 7 and 14 days (Fig. 2A). Interestingly, the overall values for OsASR5-RNAi under control condition was similar to WT plants exposed to -Fe, while OsASR5-RNAi under -Fe showed the lowest values in all three time points. There were no differences comparing time points within each genotype/treatment (Fig. 2A).

Stomatal conductance was similar to all genotypes at 7 days of treatment (Fig. 2B). At 14 days, stomatal conductance showed to be lower in OsASR5-RNAi under -Fe compared to both OsASR5-RNAi under control condition and WT under -Fe. At 21 days, stomatal conductance of OsASR5-RNAi under -Fe slightly increased but it was still lower compared to WT plants under -Fe (Fig. 2B). Consistently, OsASR5-RNAi plants under -Fe showed the highest internal CO₂ concentration (Fig. 2C). Transpiration rate was similar when comparing most genotype-treatment interactions, but OsASR5-RNAi plants exposed

to -Fe showed reduction at 14 and 21 days, both compared to 7 days after treatment (Fig. 2D). Water use efficiency (Fig. 2E) and carboxylation efficiency (Fig. 2F) showed similar patterns as found for the CO₂ assimilation rate (Fig. 2A), with OsASR5-RNAi plants with the lowest values when exposed to -Fe.

We also measured chlorophyll *a* fluorescence. Interestingly, Fv/Fm values decreased at 14 days of treatment in OsASR5-RNAi plants under -Fe and recovered at the 21st day (Fig. 2G). WT plants under -Fe, on the other hand, only showed a slight decrease at the 21st day (Fig. 2G). Few differences were observed for Fm values (Fig. 2H), while Fo was clearly increased in OsASR5-RNAi plants under -Fe at 14 days of treatment (Fig. 2I). Taken together, these data strongly suggest that while OsASR5-RNAi plants have defects in photosynthesis, -Fe exacerbates these phenotypes.

3.3. Elemental profiling of leaves and roots of OsASR5-RNAi plants

To understand whether down-regulation of OsASR genes affected the ionome, we quantified the concentrations of elements in leaves and roots of WT and OsASR5-RNAi plants under control condition and -Fe (Fig. 3). In both treatments, we observed increases in concentrations of some elements in leaves of OsASR5-RNAi plants compared to WT, such as: calcium (Ca; 72 %), copper (Cu; 81 %), manganese (Mn; 67 %), phosphorus (P; 28 %) and Fe (46 %) under control condition; and Cu (32 %), P (55 %), potassium (K; 16 %), sulphur (S; 20 %) and zinc (Zn; 31 %)

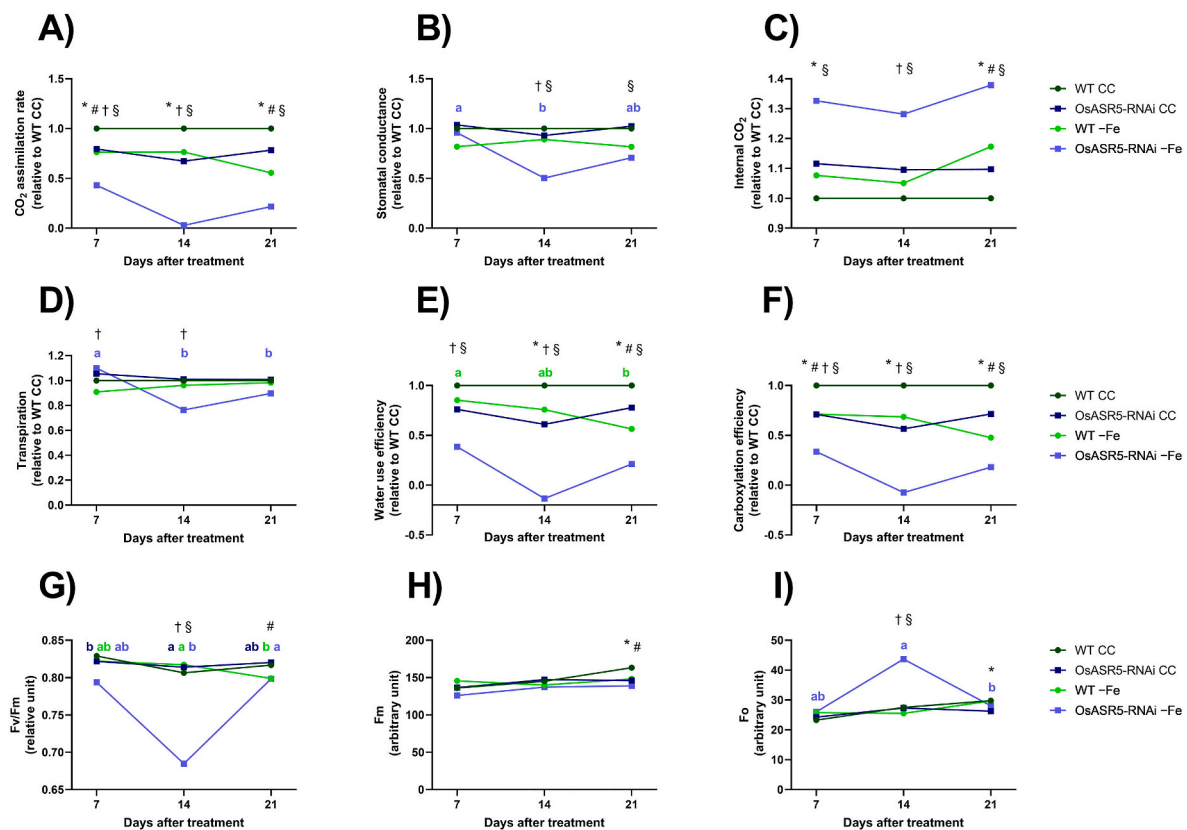


Fig. 2. The impact of *OsASR* genes knockdown and Fe deficiency treatment on photosynthesis. Changes in (A) CO₂ assimilation rate, (B) stomatal conductance, (C) internal CO₂ concentration, (D) transpiration rate, (E) water use efficiency, (F) carboxylation efficiency, (G) maximum quantum efficiency of PSII photochemistry (Fv/Fm), and (H; Fm) maximal and (I; Fo) minimal fluorescence of WT and *OsASR5*-RNAi rice plants under control condition (CC) or Fe deficiency treatment (-Fe) for 7, 14, and 21 days. All values were normalized relative to WT CC. The symbols indicate statistically significant differences determined by Student's t-test ($P \leq 0.05$) between WT CC and *OsASR5*-RNAi CC (*), WT CC and WT -Fe (#), *OsASR5*-RNAi CC and *OsASR5*-RNAi -Fe (†), or WT -Fe and *OsASR5*-RNAi -Fe (§) in each time of treatment. Different letters with the same color mean statistically significant difference comparing treatment times within the genotype-treatment group represented with the corresponding color. (For interpretation of the references to color in this figure legend, the reader is referred to the Web version of this article.)

under -Fe (Fig. 3A and B). Increases were also observed in roots of *OsASR5*-RNAi plants in both treatments: Ca (11 %), Cu (163 %), Mn (40 %) and Zn (19 %) under control condition; and Cu (94 %), Fe (94 %), Mn (48 %), P (29 %) and Zn (57 %) under -Fe (Fig. 3C and D). K was the only element to show reduced concentrations in *OsASR5*-RNAi roots in both treatments: 15 % in control condition and 28 % in -Fe (Fig. 3C and D). Furthermore, S showed a 13 % decrease only in the control condition in *OsASR5*-RNAi roots (Fig. 3C).

To understand how -Fe affect both genotypes, we also compared the ionomes of plants from the same genotype in control condition and -Fe in both leaves and roots (Fig. S1). There is an obvious decrease in Fe concentration in leaves and roots of both genotypes, as expected (Fig. S1). Interestingly, we found that P concentration is increased in *OsASR5*-RNAi leaves, but not in WT leaves, when plants are under -Fe (Figs. S1A and S1B). Zn, S, Ca, Mn and Mg decreased in WT leaves, whereas Cu and K increased (Fig. S1A). In *OsASR5*-RNAi leaves, Ca, Mn and Mg were decreased, whereas K increased by Fe deficiency (Fig. S1B). In roots, P and Mn is decreased in both genotypes, whereas Cu increased (Figs. S1C and S1D). Taken together, these results suggest that *OsASR5*-RNAi ionome changes differ from that of WT, which could be related to the -Fe chlorotic phenotype.

3.4. The knockdown of the *OsASR* genes reduces seed set and changes the seed ionome

We quantified seed set and panicle number in WT and *OsASR5*-RNAi plants. Panicle number did not differ between WT and *OsASR5*-RNAi (Fig. 4A). The total number of seeds produced by both genotypes was

similar. However, *OsASR5*-RNAi plants showed higher number of empty seeds and consequently lower number of filled seeds (Fig. 4B). We next analyzed the ionome of seeds from *OsASR5*-RNAi plants compared to WT. We found that concentrations of several elements are increased in seeds of *OsASR5*-RNAi plants other than Fe (14 %), such as K (31 %), P (25 %), magnesium (Mg; 16 %), Zn (47 %), Mn (56 %), Cu (58 %) and cadmium (Cd; 254 %) (Fig. 4C). Therefore, these data suggest that the knockdown of *OsASR* genes affects seed set in rice plants, which may also result in increased concentration of several elements in filled seeds.

3.5. Transcriptomic analyses of Fe deficiency response in *OsASR5*-RNAi plants

To gain insight into possible changes in the transcriptome of *OsASR5*-RNAi plants that can be associated with increased -Fe sensitivity, we performed RNA-seq of root tissues of both WT and *OsASR5*-RNAi plants under control condition and -Fe ($n = 3$). An average of 24.2 million pairs of reads per sample were generated and used to obtain transcript-specific expression data using Salmon (Patro et al., 2017). Approximately 87 % of the 200-bp read pairs mapped to the rice reference transcriptome *Osa1* Release 7 (Kawahara et al., 2013) (Supplementary Table S1), allowing for expression quantification of 55,683 genes (Supplementary Table S2).

The R package 3D RNA-seq was used to perform analyses of differential gene expression (Guo et al., 2021). We identified 1412 differentially expressed genes (DEGs; Supplementary Table S3 and Fig. 5A). From these, 948 genes were regulated by -Fe in WT (406 up-regulated and 542 down-regulated), while 797 genes were regulated in

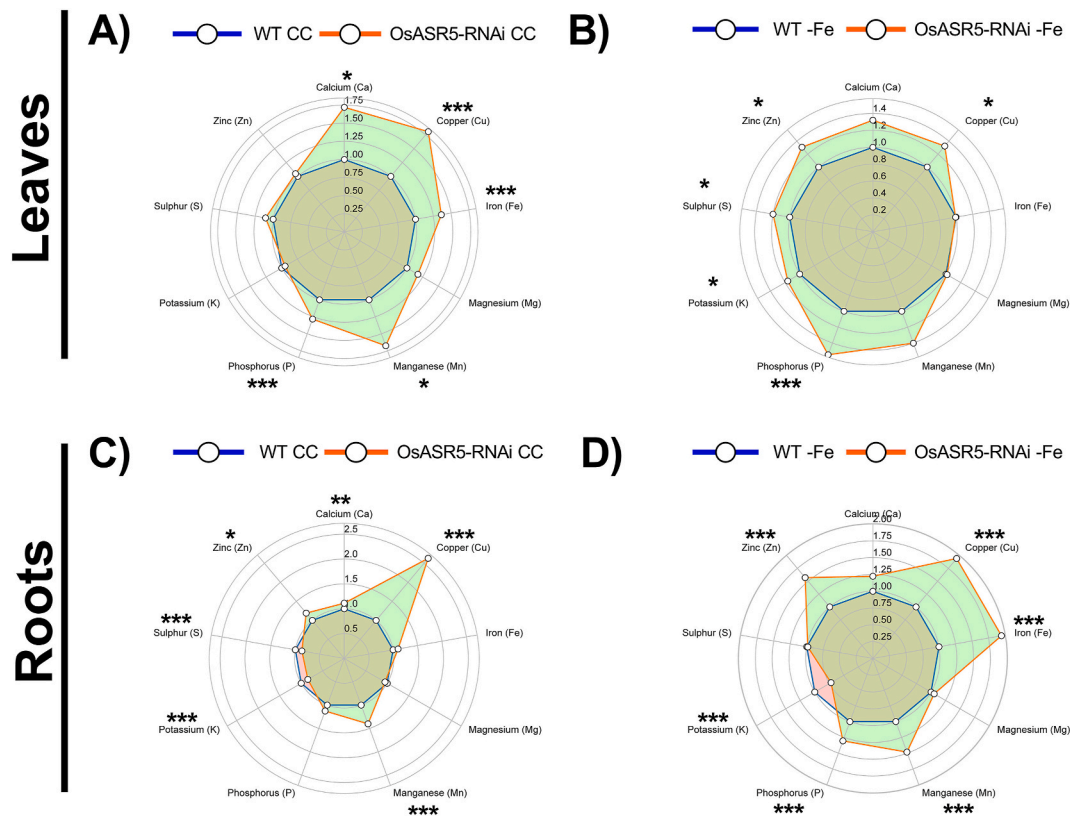


Fig. 3. Radar charts representing the average concentration ($n = 6$; $\mu\text{g g}^{-1}$ dry mass) of calcium (Ca), copper (Cu), iron (Fe), magnesium (Mg), manganese (Mn), phosphorus (P), potassium (K), sulphur (S) and zinc (Zn) in the leaves and roots of the OsASR5-RNAi line relative to the wild-type (WT) under control condition (CC) or iron deficiency ($-Fe$) at 21 days of treatment. Statistically significant differences were determined by Student's t-test (* $P \leq 0.05$; ** $P \leq 0.01$; *** $P \leq 0.001$).

OsASR5-RNAi plants (355 up-regulated and 442 down-regulated). Comparing the up-regulated gene sets, we found 288 genes commonly up-regulated in both genotypes, whereas WT plants showed 118 specific up-regulated genes, and OsASR5-RNAi plants showed 67 genes (Fig. 5B). Among the down-regulated genes, 247 were commonly down-regulated in both genotypes, whereas 295 and 195 were specific to WT and OsASR5-RNAi, respectively (Fig. 5C). These results confirm widespread transcriptomic changes in response to not only Fe deficiency but also knockdown of ASR genes in rice.

To gain insight into the pathways and functions potentially associated with the role of OsASR proteins under $-Fe$, we performed functional enrichment analysis of the DEG groups (Fig. 5B and C) using CARMO (Wang et al., 2015). A total of 22 statistically significant molecular function (MF) categories were detected for the group of genes up-regulated by Fe deficiency in both WT and OsASR5-RNAi genotypes (Fig. 6A). Among these, we found “Transporter activity”, “Metal ion transmembrane transporter activity”, “Nicotianamine synthase activity”, “Metal ion binding”, “Zinc ion transmembrane transporter activity”, “Iron ion binding” and “Iron ion transmembrane transporter activity” (Fig. 6A and Supplementary Table S4). Interestingly, eight categories were specifically enriched among up-regulated genes in WT, including “Iron ion binding”, “Oxidoreductase activity”, “ATPase activity”, “Heme binding”, “Nucleoside-triphosphatase activity” and “Transporter activity” (Fig. 6B and Supplementary Table S4). The genes exclusively up-regulated in OsASR5-RNAi plants were only enriched for “Heme binding” and “Oxidoreductase activity” (Supplementary Table S4). These results confirm that $-Fe$ significantly upregulated genes related to Fe metabolism and metals transport.

We found 27 statistically significant categories commonly enriched in down-regulated genes between WT and OsASR5-RNAi (Fig. 6C and Supplementary Table S4). Among these, we found “Oxidoreductase activity”, “Heme binding”, “Iron ion binding”, “Calcium ion binding”,

“Metal ion binding”, “Nutrient reservoir activity” and “Transporter activity”. In WT, 15 categories were specific considering the down-regulated genes, including categories such as “Iron ion binding” and “Metal ion binding” (Fig. 6D and Supplementary Table S4). In OsASR5-RNAi, 19 categories were enriched considering the down-regulated genes, including “ATP binding”, “ADP binding”, “Kinase activity”, “Nucleotide binding”, “Protein kinase activity” and “Protein serine/threonine kinase activity” (Fig. 6E and Supplementary Table S4). Taken together, these results demonstrate that, despite similarities, the two genotypes have some differences in how they respond to $-Fe$.

3.6. Differentially expressed genes under Fe deficiency in OsASR5-RNAi plants

To better understand how OsASR5-RNAi plants differ in their response to Fe deficiency compared to WT plants, we performed hierarchical clustering of all 1412 DEGs based on expression patterns, and separated them into 10 clusters (Fig. 5A and Supplementary Table S5).

Among these, we identified two clusters that contained mostly genes up-regulated by $-Fe$, regardless of the genotype: clusters 4 and 7. Cluster 4 has 196 genes, including the transcription factors *OsIRO2/OsHLH056* (Ogo et al., 2006, 2011), *OsIRO3/OsHLH063* (Li et al., 2022a; Zheng et al., 2010), *OsHLH133* (Wang et al., 2013) and *OsFIT/OsHLH156* (Wang et al., 2020); E3 ubiquitin ligase *OsHRZ2* (Guo et al., 2022; Kobayashi et al., 2013); *OsOPT7* (Bashir et al., 2015); *OsIMA1* (*IRONMAN*) (Kobayashi et al., 2021; Peng et al., 2022); *OsMIR* (de Oliveira et al., 2020; Ishimaru et al., 2009); the nicotianamine (NA)/deoxymugineic acid (DMA) transporter *OsZIFL4/OsTOM1* (Nozoye et al., 2011; Ricachenevsky et al., 2011); the two efflux transporters of NA *OsENA1* and *OsENA2/OsSTAR1* (Huang et al., 2009; Nozoye et al., 2019); and several other transporters such as *OsNRAMP1* (Curie et al., 2000), *OsIRT2* (Nakanishi et al., 2006), *OsYSL13* (Ponte

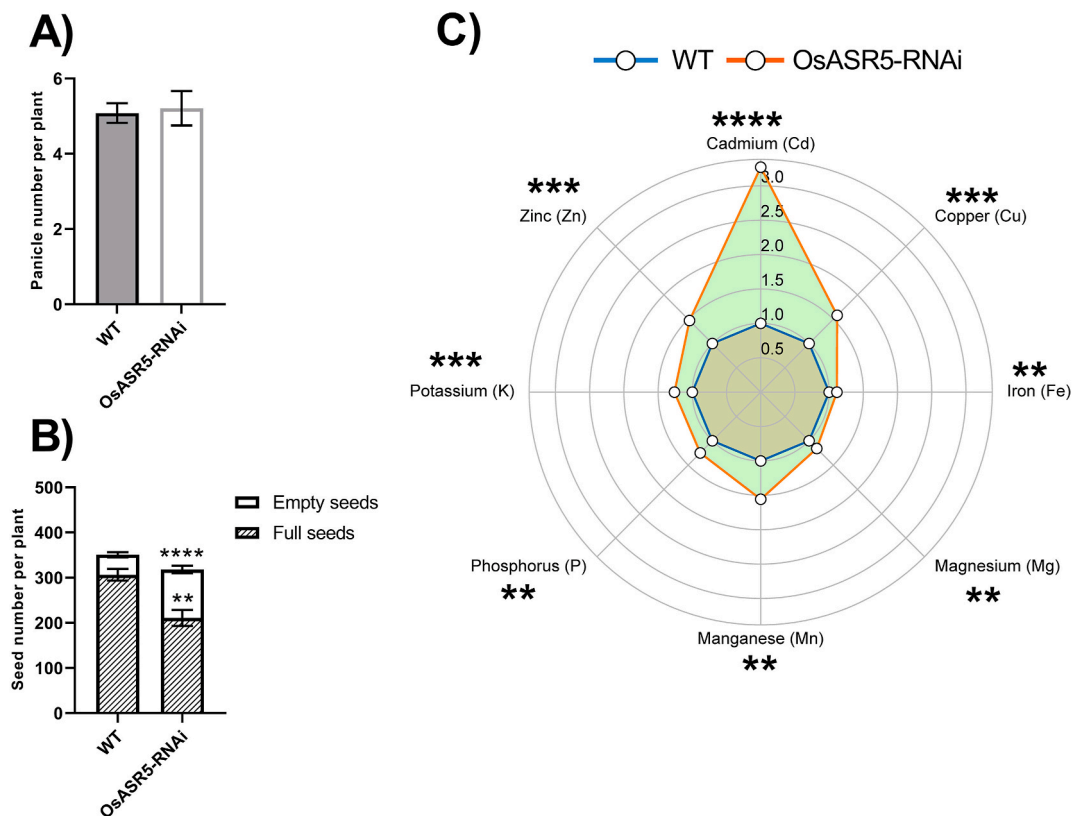


Fig. 4. The impact of *OsASR* genes knockdown on seed set and ionome composition. (A) Panicle number per plant and (B) number of filled and empty seeds per plant between WT and *OsASR5-RNAi* genotypes. (C) Radar chart representing the average concentration ($n = 5$; $\mu\text{g g}^{-1}$ dry mass) of cadmium (Cd), copper (Cu), iron (Fe), magnesium (Mg), manganese (Mn), phosphorus (P) and potassium (K) in seeds of the *OsASR5-RNAi* line relative to the wild-type (WT). Statistically significant differences were determined by Student's t-test (** $P \leq 0.01$; *** $P \leq 0.001$).

et al., 2023; Zhang et al., 2018) and *OsZIFL12/OsVMT* (Che et al., 2019; Ricachenevsky et al., 2011) (Fig. S2 and Supplementary Table S5). Genes encoding transporters for other nutrients were also identified, such as the Cu transporter *OsCOPT7* (Guan et al., 2024; Tang et al., 2024), the sulphate transporter *OsSULTR3;3* (Zhao et al., 2016) and the Zn transporter *OsZIP4* (Ishimaru et al., 2005). In addition, the arsenic (As)-responsive transporters *OsABC11* (LOC_Os01g50100) (Wang et al., 2017) and *OsMATE2* (Das et al., 2018) were also present (Fig. S2 and Supplementary Table S5). Cluster 7 has 191 genes, including other well-known genes responsive to $-Fe$ such as the E3 ubiquitin ligase *OsHRZ1* (Kobayashi et al., 2013), and important transporters, such as *OsIRT1* (Bugchio et al., 2002; Lee and An, 2009), *OsYSL15* (Inoue et al., 2009; Lee et al., 2009), *OsYSL9* (Senoura et al., 2017) and *OsPEZ2* (Bashir et al., 2011) (Fig. S3 and Supplementary Table S5).

While all genes in Cluster 4 are similarly regulated in WT and *OsASR5-RNAi* plants, 15 genes in Cluster 7 show differences in expression levels comparing the two genotypes, being either not up-regulated by $-Fe$ in *OsASR5-RNAi* plants or up-regulated to a lower extent compared to WT (Supplementary Table S5). Among these genes, we found the pleiotropic drug resistance (PDR) ABC transporter *OsPDR16/OsABCG32* (LOC_Os01g24010) (Crouzet et al., 2006; Verrier et al., 2008); a hypothetical protein encoding a small peptide (LOC_Os02g37260), a terpene synthase (LOC_Os08g07120) and the lacase gene *OsLAC23* (LOC_Os11g42200 (Liu et al., 2017);) (Fig. 7A–7D). Another eight genes are located in chromosome 7, with five located within ~ 200 kb. These include one transposon gene (LOC_Os07g25030) and four thionin-like genes, organized in two in tandem pairs (LOC_Os07g24820 and LOC_Os07g24830; LOC_Os07g25050 and LOC_Os07g25060) (Fig. 7E–7I). Moreover, *OsZIFL2* was up-regulated by $-Fe$ in WT but not in *OsASR5-RNAi* (Fig. 7J). These genes seem to be directly or indirectly dependent on *OsASR* proteins for up-regulation

under $-Fe$.

In Cluster 10, we found genes that are negatively regulated by *OsASR* proteins, since their expression was up-regulated under $-Fe$ only in *OsASR5-RNAi* plants (Fig. 5A and Supplementary Table S5). Among them, we found *OsYSL2*, a known Fe-NA transporter located in the phloem that is important for long distance Fe translocation. *OsYSL2* is induced by $-Fe$ in roots of WT plants, in agreement with data from the literature (Ishimaru et al., 2010; Koike et al., 2004). Interestingly, *OsASR5-RNAi* plants show expression levels under control condition comparable to WT under $-Fe$, and much more pronounced up-regulation under $-Fe$ (Fig. 8A). The result suggests that *OsASR5-RNAi* might not be able to adequately regulate long-distance Fe transport.

Cluster 5 contained genes down-regulated in response to $-Fe$ in both genotypes (Fig. 5A and Supplementary Table S5), including *OsFER1* and *OsFER2* (Stein et al., 2009), which are known to be positively regulated by Fe excess (Wairich et al., 2021) and negatively by $-Fe$ (Wairich et al., 2019) (Fig. 8B and C). We also observed that *OsASR* genes are grouped in Cluster 3 and Cluster 9 (Supplementary Table S5 and Supplementary Table S6). *OsASR1* and *OsASR2* are in Cluster 3. They were both down-regulated by $-Fe$ in WT, alongside *OsASR3* (Fig. 8D–8F). Intriguingly, *OsASR1* was the only *OsASR* gene to be not down-regulated in *OsASR5-RNAi* under the control condition (Fig. 8D). *OsASR3* and the three remaining *OsASR* genes, located in Cluster 9, were down-regulated in *OsASR5-RNAi* in both treatments (Fig. 8F–8I), which demonstrates that the construct is decreasing the expression of transcripts from this gene family. Altogether, these results demonstrate that *OsASR1*, *OsASR2* and *OsASR3* transcripts tend to be down-regulated in roots of WT plants under $-Fe$, and that the *OsASR5-RNAi* plants have decreased expression of *OsASR* genes, except for *OsASR1*.

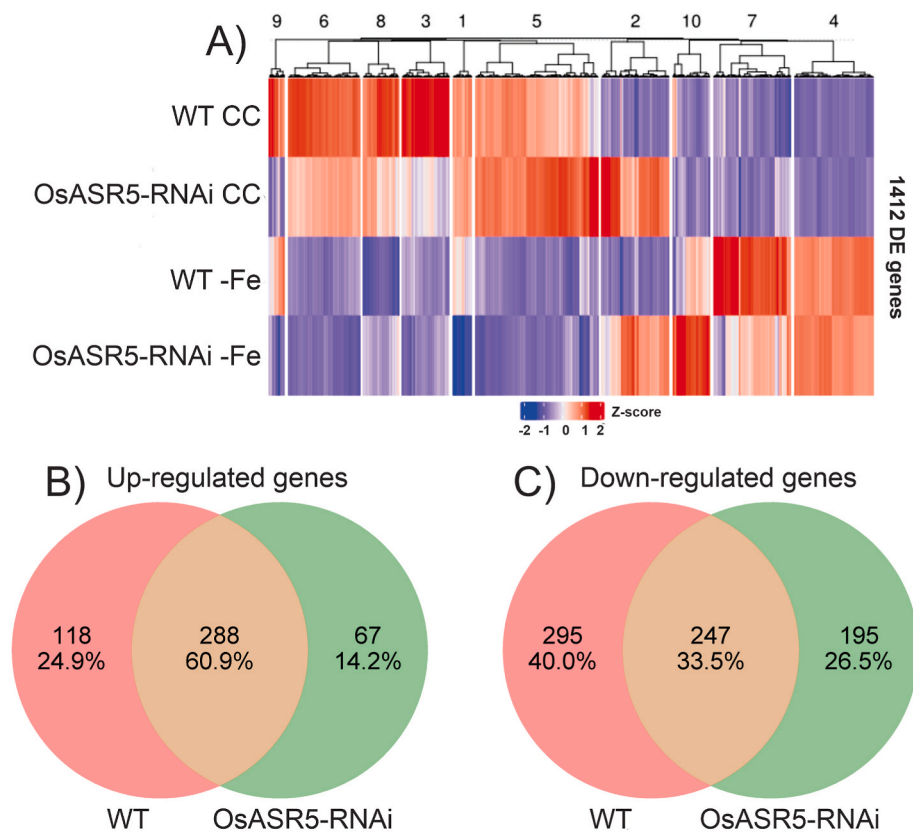


Fig. 5. Differentially expressed genes (DEGs) under Fe deficiency ($-Fe$) in both WT and OsASR5-RNAi genotypes. (A) Heatmap of 1412 DE genes between WT and OsASR5-RNAi plants under control condition (CC) or Fe deficiency ($-Fe$). (B and C) Venn diagrams showing the specific and common up- or down-regulated genes between the two genotypes under $-Fe$.

4. Discussion

ASR proteins are known to play a role in plant responses to abiotic stresses, such as drought, salinity and cold, as well as in fruit ripening regulation (Jia et al., 2016; Li et al., 2018; Parrilla et al., 2022; Yacoubi et al., 2022). Two ASR proteins from rice, OsASR1 and OsASR5, are well characterized as transcription factors and are positive regulators of genes involved in aluminum (Al) tolerance (Arenhart et al., 2013, 2014, 2016). In these studies, OsASR5-RNAi plants were more sensitive than WT to Al toxicity, as well as showing decreased transcript levels for OsASR genes (Arenhart et al., 2013). The latter is in accordance with our RNA-seq data (Fig. 8D–I; Supplementary Table S2). OsASR3 to OsASR6 showed lower expression levels in OsASR5-RNAi plants regardless of the treatment (Fig. 8F–8I; Supplementary Table S6). OsASR2 showed lower expression levels in OsASR5-RNAi only under the control condition (Fig. 8E; Supplementary Table S6). In addition, OsASR1, OsASR2 and OsASR3 showed to be down-regulated by $-Fe$ in WT plants (Fig. 8D–8F; Supplementary Table S6). Thus, our data indicate that the expression of some OsASR genes is altered regarding the Fe status of the plant.

We observed that OsASR5-RNAi plants are more sensitive to $-Fe$, showing decreased shoot growth, more pronounced chlorosis and decreased photosynthetic activity (Figs. 1 and 2). Under control condition, OsASR5-RNAi plants have increased Fe concentration in leaves, whereas under $-Fe$, OsASR5-RNAi plants leaf Fe concentration was similar to WT (Fig. 3A and B). Roots of OsASR5-RNAi plants have higher Fe concentration under $-Fe$ compared to WT (Fig. 3D). Therefore, it seems that Fe distribution in OsASR5-RNAi is disturbed, with roots retaining Fe under $-Fe$, which may be linked to lower shoot growth. It is interesting to note that P concentration is increased in OsASR5-RNAi leaves in both treatments (Fig. 3A and B), and in roots under $-Fe$ (Fig. 3D). Fe deficiency is known to increase P concentration in roots and

shoots of rice plants (Alves et al., 2025), and antagonistic interaction of Fe and P homeostasis has been extensively studied (Guo et al., 2022; Lay-Pruitt et al., 2022; Nam et al., 2021; Therby-Vale et al., 2022; Yang et al., 2024; Wairich et al., 2025). In *Arabidopsis thaliana*, $-Fe$ leads to the accumulation of ROS in the chloroplast, which triggers the down-regulation of *AtbZIP58*, a basic leucine zipper transcription factor that controls the expression of several photosynthesis-related genes (Nam et al., 2021). This results in the occurrence of $-Fe$ -induced chlorosis in leaves, which is dependent on P bioavailability. On the other hand, under combined Fe and P deficiency ($-Fe -P$), ascorbic acid accumulates in the chloroplast via the inorganic phosphate (Pi) transporter *AtPHT4; 4*, preventing the accumulation of ROS and consequently blocking the down-regulation of *AtbZIP58*. Thus, $-Fe$ -induced chlorosis is not observed in $-Fe -P$ (Nam et al., 2021). In addition, a reciprocal inhibitory module was also described between the negative regulators of Fe homeostasis, OsHRZ1 and OsHRZ2, and the central regulators of Pi signaling, OsPHR1 and OsPHR2 (PHOSPHATE STARVATION RESPONSE). Under $-Fe$, the HRZs are up-regulated both transcriptionally and translationally, which triggers the degradation of PHRs. This is supposedly a mechanism to prevent Pi accumulation from interfering with Fe root-to-shoot translocation (Guo et al., 2022). Furthermore, *phr2* and *phr1 phr2* plants were more chlorotic and had lower Fe shoot/root rates under $-Fe$ and also in $-Fe -P$. Opposite results were observed in *phr2 hrz2* plants, indicating that OsPHRs positively promote the $-Fe$ response by indirectly promoting the degradation of OsHRZs (Guo et al., 2022). Our results indicate that OsASR5-RNAi plants have higher P concentrations, which could be involved in the increased susceptibility to $-Fe$ -induced chlorosis. Further work will be necessary to explore if the mechanism involving OsPHR2/OsHRZs are linked to ASR proteins.

It is also important to mention the increases observed in the

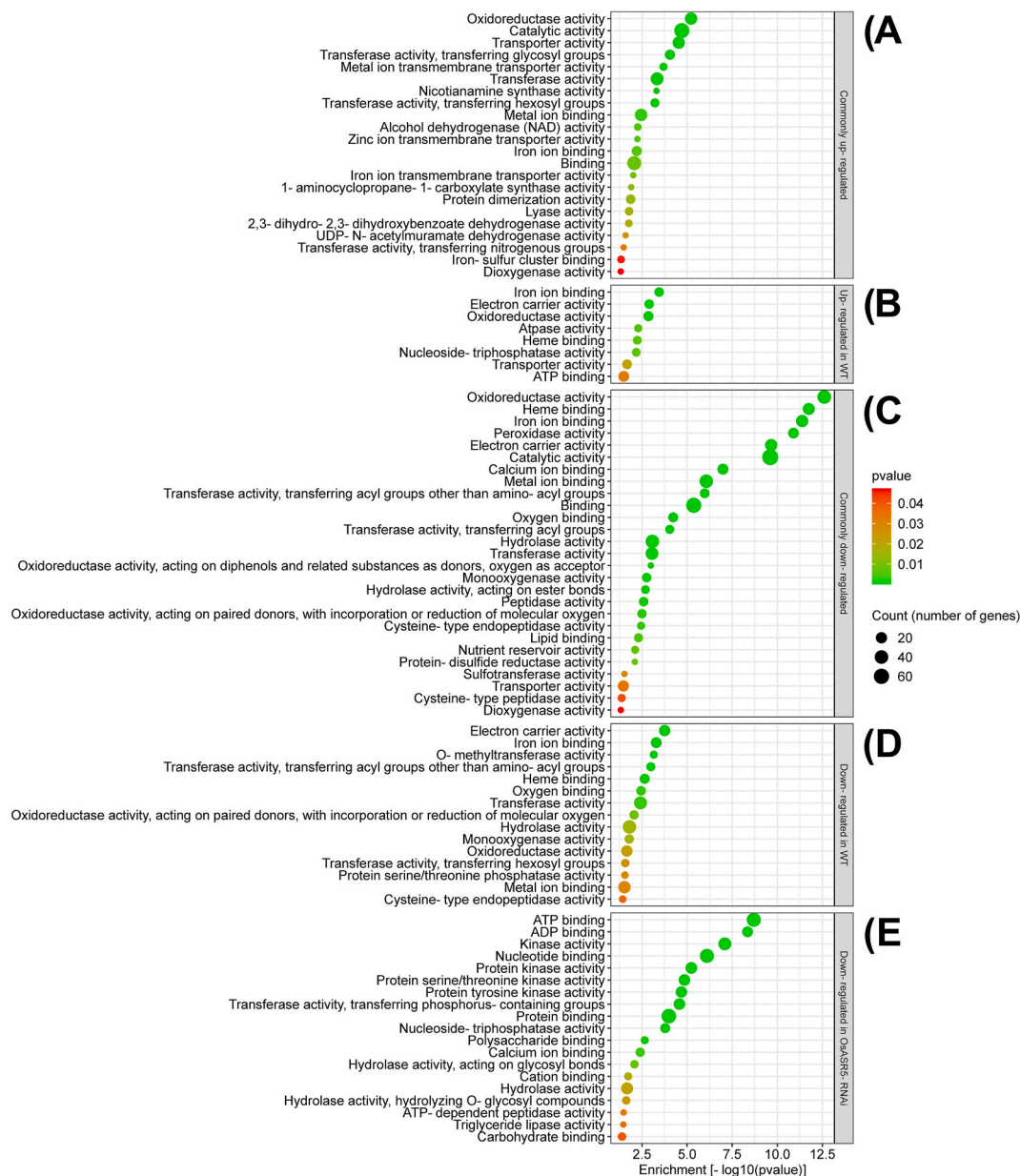


Fig. 6. Enrichment analysis of molecular functions (MF) categories of: (A) commonly up-regulated genes, (B) up-regulated genes in WT, (C) commonly down-regulated genes, (D) down-regulated genes in WT and (E) down-regulated genes in OsASR5-RNAi, comparing -Fe and control data for each genotype.

concentrations of other elements. Elemental homeostases are known to cross-talk with that of Fe by common regulatory pathways or simply by non-specific transport performed by induced divalent metal transporters (Rai et al., 2021; Wu et al., 2022; Wairich et al., 2025). Cu showed higher concentrations in the roots and leaves of OsASR5-RNAi plants under both treatments, when compared with the WT (Fig. 3). It was demonstrated that -Fe stimulates greater uptake and accumulation of Cu in different plant species (Garcia-Molina et al., 2020; Kastoori Ramamurthy et al., 2018; Waters et al., 2012; Waters and Armbrust, 2013), supposedly as a strategy for Cu/Zn superoxide dismutases (SODs) to compensate for the low levels of Fe-containing SODs in ROS scavenging (Waters et al., 2012). Regarding Zn, we observed higher concentrations in OsASR5-RNAi leaves and roots under -Fe compared to WT in the same conditions (Fig. 3B and D). Kastoori Ramamurthy et al. (2018) also observed higher Zn concentrations in Arabidopsis roots and rosettes under -Fe, but lower in comparison with the increases in Cu concentrations. It is worth noting that the Fe(II) transporter OsIRT1, which is up-regulated under -Fe, is also capable of transporting Zn,

which may explain the increases in Zn concentrations in plants subjected to -Fe (Korshunova et al., 1999; Wu et al., 2022). However, *OsIRT1* was not differentially expressed between the two genotypes in our RNA-Seq data (Fig. S3B). It will be an interesting avenue to explore how other micronutrients might be involved in OsASR5-RNAi phenotype under Fe deficiency.

Our data suggest that the mechanism by which OsASR proteins might be affecting Fe homeostasis does not involve altered Fe uptake (Kobayashi and Nishizawa, 2012). Besides *OsIRT1*, we found that -Fe markers such as *OsYSL15*, *OsIRO2*, *OsHRZ1* and *OsHRZ2*, among others (Bugchio et al., 2002; Inoue et al., 2009; Kobayashi et al., 2013; Lee et al., 2009; Lee and An, 2009), are similarly up-regulated in roots of both genotypes (Fig. S2 and Fig. S3). These data suggest that OsASR5-RNAi plants are able to properly induce the main regulatory network controlling Fe uptake, which is regulated by the transcription factor OsIDEF1 (Kobayashi et al., 2007; Kobayashi and Nishizawa, 2012). Therefore, this suggests that Fe homeostasis in OsASR5-RNAi plants is misregulated in other aspects, such as long-distance Fe transport.

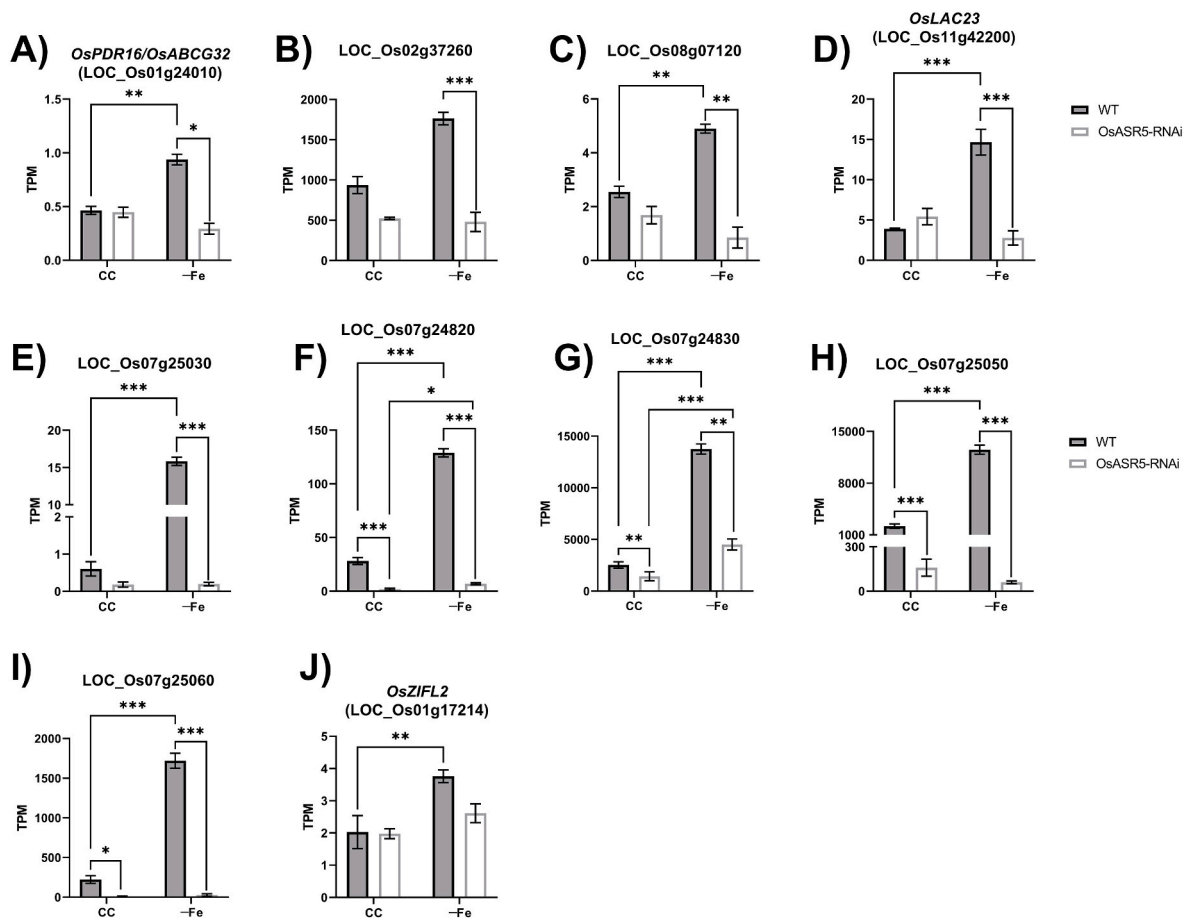


Fig. 7. Normalized expression levels from RNA-Seq of key genes located into cluster 7 under control condition (CC) or Fe deficiency (-Fe), such as (A) *OsABCG32/OsPDR16*, (B) a hypothetical protein encoding a small peptide (LOC_Os02g37260), (C) a terpene synthase (LOC_Os08g07120), (D) a laccase (LOC_Os11g42200), (E) a transposon gene (LOC_Os07g25030), (F) to (I) four thionin-like genes and (J) *OsZIFL2*. Statistically significant differences were carried out with the 3D RNA-seq app (* adjusted $P \leq 0.01$; ** adjusted $P \leq 0.001$; *** adjusted $P \leq 0.0001$). TPM, transcripts per million.

In agreement with that, *OsYSL2* expression was up-regulated in *OsASR5*-RNAi plants compared to WT, either in control condition or -Fe (Fig. 8A). *OsYSL2* is a Fe(II)/Mn(II)-NA transporter that is involved in Fe phloem long-distance transport within the plant and Fe translocation into grains (Ishimaru et al., 2010; Koike et al., 2004; Nozoye et al., 2007). Its expression is directly regulated by the NAC transcription factor IDEF2, which is constitutively expressed regardless of the Fe status of the plant (Ogo et al., 2008). Since IDEF2-*OsYSL2* regulatory module is distinct from *OsIDEF1*-*OsIRO2*-*OsYSL15* module (Kobayashi et al., 2010; Kobayashi and Nishizawa, 2012), our data suggest that *OsASR* proteins might act as a regulator of this branch of Fe deficiency response in roots.

It is also known that there is natural variation of *OsYSL2* in rice genotypes. A minor *OsYSL2* allele, named as *CF1*, was linked to Cd accumulation in grains indirectly by affecting Fe homeostasis (Li et al., 2022b). The authors observed that near isogenic lines with the high-expression, high Fe affinity *CF1*-allele, compared to the major allele, had higher concentrations of Fe in shoots and grains, while having lower concentrations of Cd. They suggested that since *CF1* has no affinity to Cd-NA, Fe status is higher in plants with the *CF1* allele, which results in decreased expression of Fe and Cd transporter *OsNRAMP5* and *OsNRAMP1*, consequently decreasing Cd translocation to aerial tissues (Ishimaru et al., 2012; Takahashi et al., 2011, 2014; Zhang et al., 2024). Although we observed higher expression of *OsYSL2* in *OsASR5*-RNAi and increased chlorosis, but no change in *OsNRAMP5* or *OsNRAMP1*, it is possible that *OsASR5*-RNAi is interfering with the regulation of *OsYSL2*, changing Fe distribution and resulting in increased chlorosis.

Moreover, we found that *OsASR* down-regulation changed the seed ionome, comparable to the phenotype observed in *CF1* minor allele-harboring plants (Li et al., 2022b). For example, we observed a substantial increase in the concentration of Cd in the grains of *OsYSL2*-up-regulated *OsASR5*-RNAi plants, when compared to WT (Fig. 4C). Higher concentration of Cd was also observed in the grains of plants carrying the high Fe affinity *CF1*-allele, suggesting that *OsASR5*-RNAi plants misregulating of *OsYSL2* might be linked to the observed seed phenotype. Taken together, these data suggest that *OsASR* proteins might be involved in the regulation of long-distance Fe transport through *OsYSL2*.

Another possible downstream candidate for *OsASR* proteins regulation is *OsZIFL2* (ZINC-INDUCED FACILITATOR LIKE) (Ricachenevsky et al., 2011). *OsZIFL2* was up-regulated by -Fe in roots of WT plants, but not in *OsASR5*-RNAi plants (Fig. 7J). The data suggest that *OsASR* proteins might be positive regulators of *OsZIFL2*. *AtZIF1* from *Arabidopsis thaliana* was the first ZIFL protein functionally characterized (Haydon et al., 2012; Haydon and Cobbett, 2007). It was shown to be a vacuolar transporter, affecting Fe and Zn homeostasis by changing NA distribution. Two paralogs, *AtZIFL1* and *AtZIFL2*, were also characterized, and it was shown that *AtZIFL1* is at least partially redundant with *AtZIF1*, whereas *AtZIFL2*, albeit also affecting Fe and Zn homeostasis, does not functionally overlap with *AtZIF1* (Lee et al., 2021). In rice and other monocots, the *ZIFL* gene family is extensively expanded (Ricachenevsky et al., 2011). This might be related to the diversification of substrates, since *Poaceae* species synthesize and use phytosiderophores (PSs) for metal uptake and movement within the plant. For

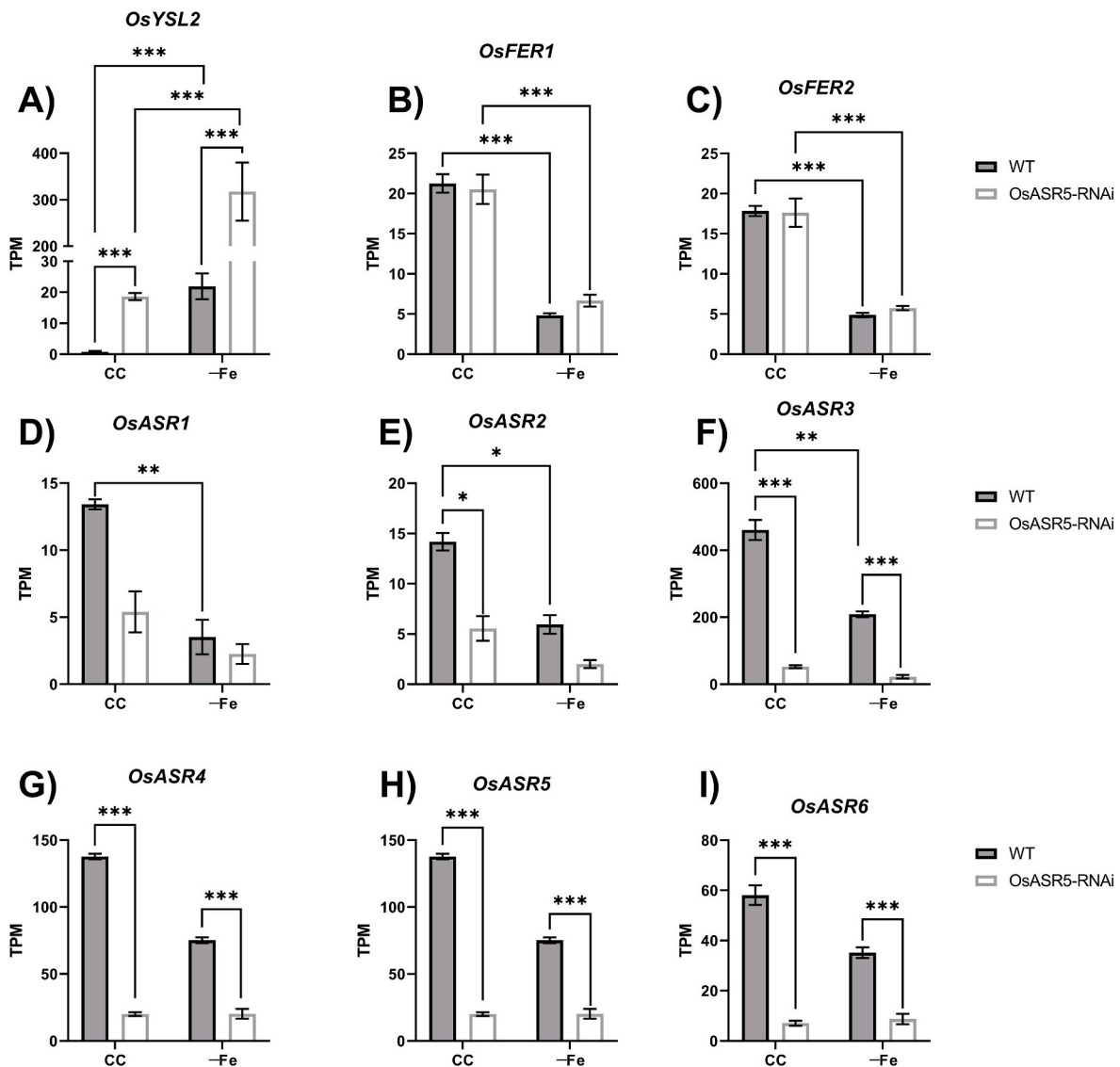


Fig. 8. Normalized expression levels from RNA-Seq of (A) *OsYSL2*, (B) *OsFER1*, (C) *OsFER2* and (D) to (I) the six rice *OsASR* genes under control condition (CC) or Fe deficiency (-Fe). Statistically significant differences were determined using the 3D RNA-seq app (* adjusted $P \leq 0.01$; ** adjusted $P \leq 0.001$; *** adjusted $P \leq 0.0001$). TPM, transcripts per million.

example, *OsZIFL4/TOM1* is a plasma-membrane-localized transporter that secretes PSs to the rhizosphere (Nozoye et al., 2011), whereas *OsZIFL12/OsVMT* is a vacuolar NA/DMA transporter (Che et al., 2019). Knockdown or knockout of either gene affects Fe homeostasis. Yet, *OsZIFL2* has no characterized function, but it is plausible that it may play a role in NA and/or PS transport within plant cells, and therefore might be involved in regulating Fe transport.

The four genes annotated as *thionins-like* (LOC_Os07g24820, LOC_Os07g24830, LOC_Os07g25050 and LOC_Os07g25060) also represent potential downstream targets of the *OsASR* proteins, since all were significantly less expressed in *OsASR5*-RNAi plants compared to the WT in -Fe (Fig. 7F–7I). To a lesser extent, the same was observed in the control condition for LOC_Os07g24820 and LOC_Os07g25050. Interestingly, LOC_Os07g24820 and LOC_Os07g24830 were expressed in *OsASR5*-RNAi under -Fe, when compared to the control condition. Thionins are small peptides that contain around 45–48 amino acid residues and have a characteristic cysteine-rich structure (Stec, 2006). They are typically known to have a broad-spectrum antimicrobial activity, which makes them important components of the plant's innate immune system against different pathogens, such as bacteria, fungi and

nematodes (Höng et al., 2021). In this sense, it is known that leguminous plants secrete small cysteine-rich peptides from roots to promote Fe sequestration. This triggers an increase in Fe uptake by bacteria, which stimulates nitrogenase, thus improving the nitrogen symbiotic fixation process (Sankari et al., 2022). In the rice genome, 44 genes coding for canonical thionins (*OsTHIONs*) were identified (Silverstein et al., 2007). To our knowledge, few rice thionin genes have been studied (Boonpa et al., 2019; Ji et al., 2015; Kitanaga et al., 2006). It was observed that the overexpression of *OsTHION9* resulted in Cd-sensitive yeast growth in media containing 10 μM or 20 μM Cd (Liu et al., 2023). *OsTHION9*-overexpressing rice plants showed higher yield per plant and reduced Cd levels in shoots and grains compared to the WT when grown in Cd-contaminated soil. The opposite results were observed in *OsTHION9*-knockout plants. Taken together, thionins and thionins-like seem to be interesting candidate genes for a possible role in Fe homeostasis and other metals.

5. Conclusions

Our work demonstrates that *ASR* proteins have a role in Fe

homeostasis. We observed decreased growth and photosynthesis, increase leaf chlorosis, and altered ionome in plants silenced for ASR genes. Transcriptomic data suggests that *OsYSL2* is misregulated in *OsASR5*-RNAi plants, suggesting that the phenotype might result from altered Fe long-distance transport. We also identified other candidate genes that might be involved in Fe deficiency sensitivity, such as putative thionin and thionin-like peptides.

Declaration of competing interest

The authors declare that there are no potential competing interests.

Acknowledgements

Authors would like to thank Conselho Nacional de Desenvolvimento Científico e Tecnológico (CNPq) for grants that supported this work (grant number 409813/2021-4 and grant number 442304/2023-4) and for fellowships to LRP and FKR. Authors also would like to thank Fundação de Amparo à Pesquisa do Estado do Rio Grande do Sul (FAPERGS) for grants that supported this work (grant number 16/2552-0000493-5). HGB received the IDEX scholarship from Université Paris-Saclay. CPGC is funded by São Paulo Research Foundation (FAPESP), grants number 2019/13158-8 and 2021/000394-5, and Institute Serrapilheira, grant number R-2011-37880. FKR is also funded by Institute Serrapilheira, grant number 1709-17256. YL-M is supported by PNPd/CAPES (Bolsista CAPES/BRASIL - Proc. 88887.473943/2020-00). This study was financed in part by the Coordenação de Aperfeiçoamento de Pessoal de Nível Superior - Brasil (CAPES) - Finance Code 001. We thank Dr. Yudelys A. Tandron Moya (Leibniz Institute of Plant Genetics and Crop Plant Research) for conducting HR-ICP-MS analysis.

Appendix A. Supplementary data

Supplementary data to this article can be found online at <https://doi.org/10.1016/j.plaphy.2025.109882>.

Data availability

Data will be made available on request.

References

- Alves, J.D.S., Menguer, P.K., Lima-Melo, Y., Fiorentini, V.H.R., Ponte, L.R., Olsson, R.V., Sasso, V.M., De Palma, N., Tabaldi, L.A., Brunetto, G., Giehl, R.F.H., Margis-Pinheiro, M., Ricachenevsky, F.K., 2025. Aluminum alleviates iron deficiency chlorosis by interfering with phosphorus homeostasis in rice (*Oryza sativa* L.). *Plant Physiol. Biochem.* 220, 109427. <https://doi.org/10.1016/j.plaphy.2024.109427>.
- Arenhart, R.A., Bai, Y., Valter de Oliveira, L.F., Bucker Neto, L., Schunemann, M., Maraschin, F., dos, S., Mariath, J., Silverio, A., Sachetto-Martins, G., Margis, R., Wang, Z.-Y., Margis-Pinheiro, M., 2014. New insights into aluminum tolerance in rice: the ASR5 protein binds the STAR1 promoter and other aluminum-responsive genes. *Mol. Plant* 7, 709–721. <https://doi.org/10.1093/mp/sst160>.
- Arenhart, R.A., Bucker-Neto, L., Margis, R., Wang, Z.-Y., Margis-Pinheiro, M., 2015. Rice Arsenal against Aluminum Toxicity, pp. 155–168. https://doi.org/10.1007/978-3-319-19968-9_8.
- Arenhart, R.A., De Lima, J.C., Pedron, M., Carvalho, F.E.L., Da Silveira, J.A.G., Rosa, S.B., Caverzan, A., Andrade, C.M.B., Schunemann, M., Margis, R., Margis-Pinheiro, M., 2013. Involvement of ASR genes in aluminum tolerance mechanisms in rice. *Plant Cell Environ.* <https://doi.org/10.1111/j.1365-3040.2012.02553.x>.
- Arenhart, R.A., Schunemann, M., Bucker Neto, L., Margis, R., Wang, Z.Y., Margis-Pinheiro, M., 2016. Rice ASR1 and ASR5 are complementary transcription factors regulating aluminum responsive genes. *Plant Cell Environ.* <https://doi.org/10.1111/pce.12655>.
- Bashir, K., Ishimaru, Y., Itai, R.N., Senoura, T., Takahashi, M., An, G., Oikawa, T., Ueda, M., Sato, A., Uozumi, N., Nakanishi, H., Nishizawa, N.K., 2015. Iron deficiency regulated *OsOPT7* is essential for iron homeostasis in rice. *Plant Mol. Biol.* 88, 165–176. <https://doi.org/10.1007/s11103-015-0315-0>.
- Bashir, K., Ishimaru, Y., Shimo, H., Kakei, Y., Senoura, T., Takahashi, R., Sato, Yutaka, Sato, Yuki, Uozumi, N., Nakanishi, H., Nishizawa, N.K., 2011. Rice phenolics efflux transporter 2 (*PEZ2*) plays an important role in solubilizing apoplasmic iron. *Soil Sci. Plant Nutr.* 57, 803–812. <https://doi.org/10.1080/00380768.2011.637305>.
- Becana, M., Moran, J.F., Iturbe-Ormaetxe, I., 1998. Iron-dependent oxygen free radical generation in plants subjected to environmental stress: toxicity and antioxidant protection. *Plant Soil* 201, 137–147. <https://doi.org/10.1023/A:1004375732137>.
- Bojórquez-Quintal, E., Escalante-Magaña, C., Echeverría-Machado, I., Martínez-Estévez, M., 2017. Aluminum, a friend or foe of higher plants in acid soils. *Front. Plant Sci.* 8. <https://doi.org/10.3389/fpls.2017.01767>.
- Bolger, A.M., Lohse, M., Usadel, B., 2014. Trimmomatic: a flexible trimmer for Illumina sequence data. *Bioinformatics* 30, 2114–2120. <https://doi.org/10.1093/bioinformatics/btu170>.
- Boonpa, K., Tantong, S., Weerawanich, K., Panpetch, P., Pringsulaka, O., Roytrakul, S., Sirikantaramas, S., 2019. In silico analyses of rice thionin genes and the antimicrobial activity of *OsTHION15* against phytopathogens. *Phytopathology* 109, 276–288. <https://doi.org/10.1094/PHYTO-06-17-0217-R>.
- Bughio, N., Yamaguchi, H., Nishizawa, N.K., Nakanishi, H., Mori, S., 2002. Cloning an iron-regulated metal transporter from rice. *J. Exp. Bot.* 53, 1677–1682. <https://doi.org/10.1093/jxb/erf004>.
- Carrillo, J.T., Borthakur, D., 2021. Methods for metal chelation in plant homeostasis: review. *Plant Physiol. Biochem.* 163, 95–107. <https://doi.org/10.1016/j.plaphy.2021.03.045>.
- Che, J., Yokosho, K., Yamaji, N., Ma, J.F., 2019. A vacuolar phytosiderophore transporter alters iron and zinc accumulation in polished rice grains. *Plant Physiol.* 181, 276–288. <https://doi.org/10.1104/pp.19.00598>.
- Connolly, E.L., Campbell, N.H., Grotz, N., Prichard, C.L., Guerinot, M. Lou, 2003. Overexpression of the FRO2 ferric chelate reductase confers tolerance to growth on low iron and uncovers posttranscriptional control. *Plant Physiol.* 133, 1102–1110. <https://doi.org/10.1104/pp.103.025122>.
- Crouzet, J., Trombik, T., Fraysse, A.S., Boutry, M., 2006. Organization and function of the plant pleiotropic drug resistance ABC transporter family. *FEBS Lett.* 580, 1123–1130. <https://doi.org/10.1016/j.febslet.2005.12.043>.
- Curie, C., Alonso, J.M., Le Jean, M., Ecker, J.R., Briat, J.F., 2000. Involvement of NRAMP1 from *Arabidopsis thaliana* in iron transport. *Biochem. J.* <https://doi.org/10.1042/0264-6021:3470749>.
- Curie, C., Panaviene, Z., Loulergue, C., Dellaporta, S.L., Briat, J.F., Walker, E.L., 2001. Maize yellow stripe1 encodes a membrane protein directly involved in Fe(III) uptake. *Nature* 409, 346–349. <https://doi.org/10.1038/35053080>.
- Das, N., Bhattacharya, S., Bhattacharyya, S., Maiti, M.K., 2018. Expression of rice MATE family transporter *OsMATE2* modulates arsenic accumulation in tobacco and rice. *Plant Mol. Biol.* 98, 101–120. <https://doi.org/10.1007/s11103-018-0766-1>.
- de Oliveira, B.H.N., Wairich, A., Turchetto-Zolet, A.C., Fett, J.P., Ricachenevsky, F.K., 2020. The Mitochondrial Iron-Regulated (MIR) gene is *Oryza* genus specific and evolved before speciation within the *Oryza sativa* complex. *Planta* 251, 94. <https://doi.org/10.1007/s00425-020-03386-2>.
- Eide, D., Broderius, M., Fett, J., Guerinot, M. Lou, 1996. A novel iron-regulated metal transporter from plants identified by functional expression in yeast. *Proc. Natl. Acad. Sci. U. S. A.* <https://doi.org/10.1073/pnas.93.11.5624>.
- Famoso, A.N., Clark, R.T., Shaff, J.E., McCouch, S.R., Kochian, L.V., 2010. Development of a novel aluminum tolerance phenotyping platform used for comparisons of cereal aluminum tolerance and investigations into rice aluminum tolerance mechanisms. *Plant Physiol.* 153, 1678–1691. <https://doi.org/10.1104/pp.110.156794>.
- García-Molina, A., Marino, G., Lehmann, M., Leister, D., 2020. Systems biology of responses to simultaneous copper and iron deficiency in *Arabidopsis*. *Plant J.* 103, 2119–2138. <https://doi.org/10.1111/tpj.14887>.
- Grillet, L., Schmidt, W., 2019. Iron acquisition strategies in land plants: not so different after all. *New Phytol.* 224, 11–18. <https://doi.org/10.1111/nph.16005>.
- Gu, Z., 2022. Complex heatmap visualization. *iMeta* 1. <https://doi.org/10.1002/imt2.43>.
- Guan, M.Y., Cao, Z., Xia, Y.C., Xv, P., Lin, X.Y., Chen, M.X., 2024. *OsCOP17* is involved in copper accumulation and transport through xylem. *J. Hazard Mater.* 477, 135245. <https://doi.org/10.1016/j.jhazmat.2024.135245>.
- Guo, M., Ruan, W., Zhang, Yibo, Zhang, Yuxin, Wang, X., Guo, Z., Wang, L., Zhou, T., Paz-Ares, J., Yi, K., 2022. A reciprocal inhibitory module for Pi and iron signaling. *Mol. Plant J.* 138–150. <https://doi.org/10.1016/j.molp.2021.09.011>.
- Guo, W., Tzioutziou, N.A., Stephen, G., Milne, I., Calixto, C.P.G., Waugh, R., Brown, J.W.S., Zhang, R., 2021. 3D RNA-seq: a powerful and flexible tool for rapid and accurate differential expression and alternative splicing analysis of RNA-seq data for biologists. *RNA Biol.* 18, 1574–1587. <https://doi.org/10.1080/15476286.2020.1858253>.
- Haydon, M.J., Cobbett, C.S., 2007. A novel major facilitator superfamily protein at the tonoplast influences zinc tolerance and accumulation in *Arabidopsis*. *Plant Physiol.* 143, 1705–1719. <https://doi.org/10.1104/pp.106.092015>.
- Haydon, M.J., Kawachi, M., Wirtz, M., Hillmer, S., Hell, R., Krämer, U., 2012. Vacuolar nicotianamine has critical and distinct roles under iron deficiency and for zinc sequestration in *Arabidopsis*. *Plant Cell* 24, 724–737. <https://doi.org/10.1105/tpc.111.095042>.
- Höng, K., Austerlitz, T., Bohlmann, T., Bohlmann, H., 2021. The thionin family of antimicrobial peptides. *PLoS One* 16, e0254549. <https://doi.org/10.1371/journal.pone.0254549>.
- Huang, C.F., Yamaji, N., Mitani, N., Yano, M., Nagamura, Y., Ma, J.F., 2009. A bacterial-type ABC transporter is involved in aluminum tolerance in rice. *Plant Cell* 21, 655–667. <https://doi.org/10.1105/tpc.108.064543>.
- Huang, T., Suen, D., 2021. Iron insufficiency in floral buds impairs pollen development by disrupting tapetum function. *Plant J.* 108, 244–267. <https://doi.org/10.1111/tpj.15438>.
- Inoue, H., Kobayashi, T., Nozoye, T., Takahashi, M., Kakei, Y., Suzuki, K., Nakazono, M., Nakanishi, H., Mori, S., Nishizawa, N.K., 2009. Rice *OsYSL15* is an iron-regulated iron (III)-deoxymugineic acid transporter expressed in the roots and is essential for

- iron uptake in early growth of the seedlings. *J. Biol. Chem.* 284, 3470–3479. <https://doi.org/10.1074/jbc.M806042200>.
- Ishimaru, Y., Bashir, K., Fujimoto, M., An, G., Itai, R.N., Tsutsumi, N., Nakanishi, H., Nishizawa, N.K., 2009. Rice-specific mitochondrial iron-regulated gene (MIR) plays an important role in iron homeostasis. *Mol. Plant* 2, 1059–1066. <https://doi.org/10.1093/mp/ssp051>.
- Ishimaru, Y., Bashir, K., Nakanishi, H., Nishizawa, N.K., 2012. OsNRAMP5, a major player for constitutive iron and manganese uptake in rice. *Plant Signal. Behav.* 7, 763–766. <https://doi.org/10.4161/psb.20510>.
- Ishimaru, Y., Masuda, H., Bashir, K., Inoue, H., Tsukamoto, T., Takahashi, M., Nakanishi, H., Aoki, N., Hirose, T., Ohsugi, R., Nishizawa, N.K., 2010. Rice metal-nicotianamine transporter, OsYSL2, is required for the long-distance transport of iron and manganese. *Plant J.* 62, 379–390. <https://doi.org/10.1111/j.1365-313X.2010.04158.x>.
- Ishimaru, Y., Suzuki, M., Kobayashi, T., Takahashi, M., Nakanishi, H., Mori, S., Nishizawa, N.K., 2005. OsZIP4, a novel zinc-regulated zinc transporter in rice. *J. Exp. Bot.* 56, 3207–3214. <https://doi.org/10.1093/jxb/eri317>.
- Ishimaru, Y., Suzuki, M., Tsukamoto, T., Suzuki, K., Nakazono, M., Kobayashi, T., Wada, Y., Watanabe, S., Matsuhashi, S., Takahashi, M., Nakanishi, H., Mori, S., Nishizawa, N.K., 2006. Rice plants take up iron as an Fe³⁺-phytosiderophore and as Fe²⁺. *Plant J.* 45, 335–346. <https://doi.org/10.1111/j.1365-313X.2005.02624.x>.
- Ji, H., Gheysen, G., Ullah, C., Verbeek, R., Shang, C., De Vleeschauwer, D., Höfte, M., Kyndt, T., 2015. The role of thionins in rice defence against root pathogens. *Mol. Plant Pathol.* 16, 870–881. <https://doi.org/10.1111/mpp.12246>.
- Jia, H., Jiu, S., Zhang, C., Wang, C., Tariq, P., Liu, Z., Wang, B., Cui, L., Fang, J., 2016. Abscisic acid and sucrose regulate tomato and strawberry fruit ripening through the abscisic acid-stress-ripening transcription factor. *Plant Biotechnol. J.* 14, 2045–2065. <https://doi.org/10.1111/pbi.12563>.
- Kastoori Ramamurthy, R., Xiang, Q., Hsieh, E.-J., Liu, K., Zhang, C., Waters, B.M., 2018. New aspects of iron–copper crosstalk uncovered by transcriptomic characterization of Col-0 and the copper uptake mutant spl7 in *Arabidopsis thaliana*. *Metallomics* 10, 1824–1840. <https://doi.org/10.1039/C8MT00287H>.
- Kawahara, Y., de la Bastide, M., Hamilton, J.P., Kanamori, H., McCombie, W.R., Ouyang, S., Schwartz, D.C., Tanaka, T., Wu, J., Zhou, S., Childs, K.L., Davidson, R. M., Lin, H., Quesada-Ocampo, L., Vaillancourt, B., Sakai, H., Lee, S.S., Kim, J., Numa, H., Itoh, T., Buell, C.R., Matsumoto, T., 2013. Improvement of the *Oryza sativa* Nipponbare reference genome using next generation sequence and optical map data. *Rice* 6, 4. <https://doi.org/10.1186/1939-8433-6-4>.
- Kim, S.T., Kim, S.G., Agrawal, G.K., Kikuchi, S., Rakwal, R., 2014. Rice proteomics: a model system for crop improvement and food security. *Proteomics* 14, 593–610. <https://doi.org/10.1002/pmic.201300388>.
- Kitanaga, Y., Jian, C., Hasegawa, M., Yazaki, J., Kishimoto, N., Kikuchi, S., Nakamura, H., Ichikawa, H., Asami, T., Yoshida, S., Yamaguchi, I., Suzuki, Y., 2006. Sequential regulation of gibberellin, brassinosteroid, and jasmonic acid biosynthesis occurs in rice coleoptiles to control the transcript levels of anti-microbial thionin genes. *Biosci. Biotechnol. Biochem.* 70, 2410–2419. <https://doi.org/10.1271/bbb.60145>.
- Kobayashi, T., Nagano, A.J., Nishizawa, N.K., 2021. Iron deficiency-inducible peptide-coding genes OsIMA1 and OsIMA2 positively regulate a major pathway of iron uptake and translocation in rice. *J. Exp. Bot.* 72, 2196–2211. <https://doi.org/10.1093/jxb/era546>.
- Kobayashi, T., Nagasaka, S., Senoura, T., Itai, R.N., Nakanishi, H., Nishizawa, N.K., 2013. Iron-binding haemerythrin RING ubiquitin ligases regulate plant iron responses and accumulation. *Nat. Commun.* 4, 2792. <https://doi.org/10.1038/ncomms3792>.
- Kobayashi, T., Nishizawa, N.K., 2012. Iron uptake, translocation, and regulation in higher plants. *Annu. Rev. Plant Biol.* 63, 131–152. <https://doi.org/10.1146/annurev-arplant-042811-105522>.
- Kobayashi, T., Ogo, Y., Aung, M.S., Nozoye, T., Itai, R.N., Nakanishi, H., Yamakawa, T., Nishizawa, N.K., 2010. The spatial expression and regulation of transcription factors IDEF1 and IDEF2. *Ann. Bot.* 105, 1109–1117. <https://doi.org/10.1093/aob/mcq002>.
- Kobayashi, T., Ogo, Y., Itai, R.N., Nakanishi, H., Takahashi, M., Mori, S., Nishizawa, N.K., 2007. The transcription factor IDEF1 regulates the response to and tolerance of iron deficiency in plants. *Proc. Natl. Acad. Sci.* 104, 19150–19155. <https://doi.org/10.1073/pnas.0707010104>.
- Koike, S., Inoue, H., Mizuno, D., Takahashi, M., Nakanishi, H., Mori, S., Nishizawa, N.K., 2004. OsYSL2 is a rice metal-nicotianamine transporter that is regulated by iron and expressed in the phloem. *Plant J.* 39, 415–424. <https://doi.org/10.1111/j.1365-313X.2004.02146.x>.
- Korshunova, Y.O., Eide, D., Clark, W.G., Guerinot, M. Lou, Pakrasi, H.B., 1999. The IRT1 protein from *Arabidopsis thaliana* is a metal transporter with a broad substrate range. *Plant Mol. Biol.* 40, 37–44. <https://doi.org/10.1023/a:1026438615520>.
- Krohling, C.A., Eutrópio, F.J., Bertolazi, A.A., Dobbs, L.B., Campostri, E., Dias, T., Ramos, A.C., 2016. Ecophysiology of iron homeostasis in plants. *Soil Sci. Plant Nutr.* 62, 39–47. <https://doi.org/10.1080/00380768.2015.1123116>.
- Lay-Pruitt, K.S., Wang, W., Prom-u-thai, C., Pandey, A., Zheng, L., Rouached, H., 2022. A tale of two players: the role of phosphate in iron and zinc homeostatic interactions. *Planta* 256, 23. <https://doi.org/10.1007/s00425-022-03922-2>.
- Lee, S., An, G., 2009. Over-expression of OsIRT1 leads to increased iron and zinc accumulations in rice. *Plant Cell Environ.* 32, 408–416. <https://doi.org/10.1111/j.1365-3040.2009.01935.x>.
- Lee, S., Chiecko, J.C., Kim, S.A., Walker, E.L., Lee, Y., Guerinot, M.L., An, G., 2009. Disruption of OsYSL15 leads to iron inefficiency in rice plants. *Plant Physiol.* 150, 786–800. <https://doi.org/10.1104/pp.109.135418>.
- Lee, S., Ricachenevsky, F.K., Punshon, T., 2021. Functional overlap of two major facilitator superfamily transporter, ZIF1, and ZIFL1 in zinc and iron homeostasis. *Biochem. Biophys. Res. Commun.* 560, 7–13. <https://doi.org/10.1016/j.bbrc.2021.04.120>.
- Li, C., Li, Y., Xu, P., Liang, G., 2022a. OsIRO3 negatively regulates Fe homeostasis by repressing the expression of OsIRO2. *Plant J.* 111, 966–978. <https://doi.org/10.1111/tpj.15864>.
- Li, X., Li, L., Zuo, S., Li, J., Wei, S., 2018. Differentially expressed ZmASR genes associated with chilling tolerance in maize (*Zea mays*) varieties. *Funct. Plant Biol.* 45, 1173. <https://doi.org/10.1071/FP17356>.
- Liu, Q., Luo, L., Wang, X., Shen, Z., Zheng, L., 2017. Comprehensive analysis of rice laccase gene (OsLAC) family and ectopic expression of OsLAC10 enhances tolerance to copper stress in *Arabidopsis*. *Int. J. Mol. Sci.* 18, 209. <https://doi.org/10.3390/ijms18020209>.
- Li, L., Mao, D., Sun, L., Wang, R., Tan, L., Zhu, Y., Huang, H., Peng, C., Zhao, Y., Wang, J., Huang, D., Chen, C., 2022b. CF1 reduces grain-cadmium levels in rice (*Oryza sativa*). *Plant J.* 110, 1305–1318. <https://doi.org/10.1111/tpj.15736>.
- Liu, X., Gong, X., Zhou, B., Jiang, Q., Liang, Y., Ye, R., Zhang, S., Wang, Y., Tang, X., Li, F., Yi, J., 2023. Plant defensin-dissimilar thionin OsThi9 alleviates cadmium toxicity in rice plants and reduces cadmium accumulation in rice grains. *J. Agric. Food Chem.* 71, 8367–8380. <https://doi.org/10.1021/acs.jafc.3c01032>.
- Liu, Y., Xiong, Z., Wu, W., Ling, H.-Q., Kong, D., 2023. Iron in the symbiosis of plants and microorganisms. *Plants* 12, 1958. <https://doi.org/10.3390/plants12101958>.
- Nakanishi, H., Ogo, Y., Ishimaru, Y., Mori, S., Nishizawa, N.K., 2006. Iron deficiency enhances cadmium uptake and translocation mediated by the Fe²⁺ transporters OsIRT1 and OsIRT2 in rice. *Soil Sci. Plant Nutr.* 52, 464–469. <https://doi.org/10.1111/j.1747-0765.2006.00055.x>.
- Nam, H.-I., Shahzad, Z., Dorone, Y., Clowez, S., Zhao, K., Bouain, N., Lay-Pruitt, K.S., Cho, H., Rhee, S.Y., Rouached, H., 2021. Interdependent iron and phosphorus availability controls photosynthesis through retrograde signaling. *Nat. Commun.* 12, 7211. <https://doi.org/10.1038/s41467-021-27548-2>.
- Nozoye, T., Inoue, H., Takahashi, M., Ishimaru, Y., Nakanishi, H., Mori, S., Nishizawa, N.K., 2007. The expression of iron homeostasis-related genes during rice germination. *Plant Mol. Biol.* 64, 35–47. <https://doi.org/10.1007/s11103-007-9132-4>.
- Nozoye, T., Nagasaka, S., Kobayashi, T., Takahashi, M., Sato, Yuki, Sato, Yoko, Uozumi, N., Nakanishi, H., Nishizawa, N.K., 2011. Phytosiderophore efflux transporters are crucial for iron acquisition in graminaceous plants. *J. Biol. Chem.* 286, 5446–5454. <https://doi.org/10.1074/jbc.M110.180026>.
- Nozoye, T., von Wirén, N., Sato, Y., Higashiyama, T., Nakanishi, H., Nishizawa, N.K., 2019. Characterization of the nicotianamine exporter ENA1 in rice. *Front. Plant Sci.* 10. <https://doi.org/10.3389/fpls.2019.00502>.
- Ogo, Y., Itai, R.N., Kobayashi, T., Aung, M.S., Nakanishi, H., Nishizawa, N.K., 2011. OsIRO2 is responsible for iron utilization in rice and improves growth and yield in calcareous soil. *Plant Mol. Biol.* 75, 593–605. <https://doi.org/10.1007/s11103-011-9752-6>.
- Ogo, Y., Itai, R.N., Nakanishi, H., Inoue, H., Kobayashi, T., Suzuki, M., Takahashi, M., Mori, S., Nishizawa, N.K., 2006. Isolation and characterization of IRO2, a novel iron-regulated bHLH transcription factor in graminaceous plants. *J. Exp. Bot.* 57, 2867–2878. <https://doi.org/10.1093/jxb/erl054>.
- Ogo, Y., Kobayashi, T., Nakanishi, H., Kakei, Y., Takahashi, M., Toki, S., Mori, S., Nishizawa, N.K., 2008. A novel NAC transcription factor, IDEF2, that recognizes the iron deficiency-responsive element 2 regulates the genes involved in iron homeostasis in plants. *J. Biol. Chem.* 283, 13407–13417. <https://doi.org/10.1074/jbc.M708732200>.
- Parrilla, J., Medici, A., Gaillard, C., Verbeke, J., Gibon, Y., Rolin, D., Laloui, M., Finkelstein, R.R., Atanassova, R., 2022. Grape ASR regulates glucose transport, metabolism and signaling. *Int. J. Mol. Sci.* 23, 6194. <https://doi.org/10.3390/ijms23116194>.
- Patro, R., Duggal, G., Love, M.I., Irizarry, R.A., Kingsford, C., 2017. Salmon provides fast and bias-aware quantification of transcript expression. *Nat. Methods* 14, 417–419. <https://doi.org/10.1038/nmeth.4197>.
- Peng, F., Li, C., Lu, C., Li, Y., Xu, P., Liang, G., 2022. IRONMAN peptide interacts with OsHRZ1 and OsHRZ2 to maintain Fe homeostasis in rice. *J. Exp. Bot.* 73, 6463–6474. <https://doi.org/10.1093/jxb/erac299>.
- Philippe, R., Courtois, B., McNally, K.L., Mournet, P., El-Malki, R., Le Paslier, M.C., Fabre, D., Billot, C., Brunel, D., Glaszmann, J.-C., This, D., 2010. Structure, allelic diversity and selection of Asr genes, candidate for drought tolerance, in *Oryza sativa* L. and wild relatives. *Theor. Appl. Genet.* 121, 769–787. <https://doi.org/10.1007/s00122-010-1348-z>.
- Ponte, L.R., Farias, J.G., Del Frari, B.K., Costa, H.K., Prigol, L.H.F., Caye, M., Fett, J.P., Hanzel, F.B., Dressler, V.L., Sperotto, R.A., Brunetto, G., Ricachenevsky, F.K., 2023. OsYSL13 transporter may play a role in Mn homeostasis in rice (*Oryza sativa* L.). *Theor. Exp. Plant Physiol.* <https://doi.org/10.1007/s40626-023-00282-4>.
- Przybyla-Toscano, J., Boussard, C., Law, S.R., Rouhier, N., Keech, O., 2021. Gene atlas of iron-containing proteins in *Arabidopsis thaliana*. *Plant J.* 106, 258–274. <https://doi.org/10.1111/tpj.15154>.
- Rai, S., Singh, P.K., Mankotia, S., Swain, J., Satbhai, S.B., 2021. Iron homeostasis in plants and its crosstalk with copper, zinc, and manganese. *Plant Stress* 1, 100008. <https://doi.org/10.1016/j.stress.2021.100008>.
- Ranjan, A., Sinha, R., Sharma, T.R., Pattanayak, A., Singh, A.K., 2021. Alleviating aluminum toxicity in plants: implications of reactive oxygen species signaling and crosstalk with other signaling pathways. *Physiol. Plantarum* 173, 1765–1784. <https://doi.org/10.1111/ppl.13382>.
- Ricachenevsky, F.K., Sperotto, R.A., Menguer, P.K., Sperb, E.R., Lopes, K.L., Fett, J.P., 2011. ZINC-INDUCED FACILITATOR-LIKE family in plants: lineage-specific expansion in monocotyledons and conserved genomic and expression features among rice (*Oryza sativa*) paralogs. *BMC Plant Biol.* 11, 20. <https://doi.org/10.1186/1471-2229-11-20>.

- Robinson, N.J., Procter, C.M., Connolly, E.L., Guerinot, M. Lou, 1999. A ferric-chelate reductase for iron uptake from soils. *Nature* 397, 694–697. <https://doi.org/10.1038/17800>.
- Rodrigues, W.F.C., Lisboa, A.B.P., Lima, J.E., Ricachenevsky, F.K., Del-Bem, L., 2023. Ferric iron uptake via IRT1/ZIP evolved at least twice in green plants. *New Phytol.* 237, 1951–1961. <https://doi.org/10.1111/nph.18661>.
- Sankari, S., Babu, V.M.P., Bian, K., Alhazmi, A., Andorfer, M.C., Avalos, D.M., Smith, T. A., Yoon, K., Drennan, C.L., Yaffe, M.B., Lourido, S., Walker, G.C., 2022. A haem-sequestering plant peptide promotes iron uptake in symbiotic bacteria. *Nat. Microbiol.* 7, 1453–1465. <https://doi.org/10.1038/s41564-022-01192-y>.
- Saraçlı, S., Doğan, N., Doğan, İ., 2013. Comparison of hierarchical cluster analysis methods by cophenetic correlation. *J. Inequalities Appl.* 2013, 203. <https://doi.org/10.1186/1029-242X-2013-203>.
- Schreiber, U., Endo, T., Mi, H., Asada, K., 1995. Quenching analysis of chlorophyll fluorescence by the saturation pulse method: particular aspects relating to the study of eukaryotic algae and cyanobacteria. *Plant Cell Physiol.* 36, 873–882. <https://doi.org/10.1093/oxfordjournals.pcp.a078833>.
- Senoura, T., Sakashita, E., Kobayashi, T., Takahashi, M., Aung, M.S., Masuda, H., Nakanishi, H., Nishizawa, N.K., 2017. The iron-chelate transporter OsYSL9 plays a role in iron distribution in developing rice grains. *Plant Mol. Biol.* <https://doi.org/10.1007/s11103-017-0656-y>.
- Silverstein, K.A.T., Moskal, W.A., Wu, H.C., Underwood, B.A., Graham, M.A., Town, C. D., VandenBosch, K.A., 2007. Small cysteine-rich peptides resembling antimicrobial peptides have been under-predicted in plants. *Plant J.* 51, 262–280. <https://doi.org/10.1111/j.1365-313X.2007.03136.x>.
- Song, S., Tian, D., Zhang, Z., Hu, S., Yu, J., 2018. Rice genomics: over the past two decades and into the future. *Genom. Proteom. Bioinform.* 16, 397–404. <https://doi.org/10.1016/j.gpb.2019.01.001>.
- Stec, B., 2006. Plant thionins – the structural perspective. *Cell. Mol. Life Sci.* 63, 1370–1385. <https://doi.org/10.1007/s00018-005-5574-5>.
- Stein, R.J., Duarte, G.L., Scheunemann, L., Spohr, M.G., de Araujo Júnior, A.T., Ricachenevsky, F.K., Rosa, L.M.G., Zanchin, N.I.T., Santos, R.P. dos, Fett, J.P., 2019. Genotype variation in rice (*Oryza sativa* L.) tolerance to Fe toxicity might be linked to root cell wall lignification. *Front. Plant Sci.* 10. <https://doi.org/10.3389/fpls.2019.00746>.
- Stein, R.J., Ricachenevsky, F.K., Fett, J.P., 2009. Differential regulation of the two rice ferritin genes (OsFER1 and OsFER2). *Plant Sci.* 177, 563–569. <https://doi.org/10.1016/j.plantsci.2009.08.001>.
- Takahashi, R., Ishimaru, Y., Senoura, T., Shimo, H., Ishikawa, S., Arai, T., Nakanishi, H., Nishizawa, N.K., 2011. The OsNRAMP1 iron transporter is involved in Cd accumulation in rice. *J. Exp. Bot.* 62, 4843–4850. <https://doi.org/10.1093/jxb/err136>.
- Takahashi, R., Ishimaru, Y., Shimo, H., Bashir, K., Senoura, T., Sugimoto, K., Ono, K., Suzui, N., Kawachi, N., Ishii, S., Yin, Y.-G., Fujimaki, S., Yano, M., Nishizawa, N.K., Nakanishi, H., 2014. From laboratory to field: OsNRAMP5-knockdown rice is a promising candidate for Cd phytoremediation in paddy fields. *PLoS One* 9, e98816. <https://doi.org/10.1371/journal.pone.0098816>.
- Tang, D., Chen, M., Huang, X., Zhang, Guicheng, Zeng, L., Zhang, Guangsen, Wu, S., Wang, Y., 2023. SRplot: a free online platform for data visualization and graphing. *PLoS One* 18, e0294236. <https://doi.org/10.1371/journal.pone.0294236>.
- Tang, Z., Li, Y., Zhang, Z., Huang, X., Zhao, F., 2024. OsCOPT7 is a copper exporter at the tonoplast and endoplasmic reticulum and controls Cu translocation to the shoots and grain of rice. *Plant Cell Environ.* 47, 2163–2177. <https://doi.org/10.1111/pce.14867>.
- Therby-Vale, R., Lacombe, B., Rhee, S.Y., Nussaume, L., Rouached, H., 2022. Mineral nutrient signaling controls photosynthesis: focus on iron deficiency-induced chlorosis. *Trends Plant Sci.* 27, 502–509. <https://doi.org/10.1016/j.tplants.2021.11.005>.
- Trofimov, K., Mankotia, S., Ngigi, M., Baby, D., Satbhai, S.B., Bauer, P., 2024. Shedding light on iron nutrition: exploring intersections of transcription factor cascades in light and iron deficiency signaling. *J. Exp. Bot.* <https://doi.org/10.1093/jxb/erae324>.
- Verrier, P.J., Bird, D., Burla, B., Dassa, E., Forestier, C., Geisler, M., Klein, M., Kolukisaoglu, Ü., Lee, Y., Martinoia, E., Murphy, A., Rea, P.A., Samuels, L., Schulz, B., Spalding, E.P., Yazaki, K., Theodoulou, F.L., 2008. Plant ABC proteins – a unified nomenclature and updated inventory. *Trends Plant Sci.* 13, 151–159. <https://doi.org/10.1016/j.tplants.2008.02.001>.
- Vert, G., Grotz, N., Dédaldéchamp, F., Gaymard, F., Guerinot, M. Lou, Briat, J.-F., Curie, C., 2002. IRT1, an Arabidopsis transporter essential for iron uptake from the soil and for plant growth. *Plant Cell* 14, 1223–1233. <https://doi.org/10.1105/tpc.001388>.
- Vitoriano, C.B., Calixto, C.P.G., 2021. Reading between the lines: RNA-seq data mining reveals the alternative message of the rice leaf transcriptome in response to heat stress. *Plants* 10, 1647. <https://doi.org/10.3390/plants10081647>.
- Wairich, A., Aung, M.S., Ricachenevsky, F.K., Masuda, H., 2024. You can't always get as much iron as you want: how rice plants deal with excess of an essential nutrient. *Front. Plant Sci.* 15. <https://doi.org/10.3389/fpls.2024.1381856>.
- Wairich, A., de Oliveira, B.H.N., Arend, E.B., Duarte, G.L., Ponte, L.R., Sperotto, R.A., Ricachenevsky, F.K., Fett, J.P., 2019. The Combined Strategy for iron uptake is not exclusive to domesticated rice (*Oryza sativa*). *Sci. Rep.* <https://doi.org/10.1038/s41598-019-52502-0>.
- Wairich, A., De Oliveira, B.H.N., Wu, L.B., Murugaiyan, V., Margis-Pinheiro, M., Fett, J. P., Ricachenevsky, F.K., Frei, M., 2021. Chromosomal introgressions from *Oryza meridionalis* into domesticated rice *Oryza sativa* result in iron tolerance. *J. Exp. Bot.* <https://doi.org/10.1093/jxb/erae461>.
- Wairich, A., Ricachenevsky, F.K., Lee, S., 2022. A tale of two metals: biofortification of rice grains with iron and zinc. *Front. Plant Sci.* 13. <https://doi.org/10.3389/fpls.2022.944624>.
- Wairich, A., Lima-Melo, Y., Menguer, P.K., Ortolan, F., Ricachenevsky, F.K., 2025. Iron, cold iron, is the master of them all: iron crosstalk with zinc, copper, phosphorus and nitrogen homeostasis. *J. Exp. Bot.* <https://doi.org/10.1093/jxb/eraf106>.
- Wang, F.-Z., Chen, M.-X., Yu, L.-J., Xie, L.-J., Yuan, L.-B., Qi, H., Xiao, M., Guo, W., Chen, Z., Yi, K., Zhang, J., Qiu, R., Shu, W., Xiao, S., Chen, Q.-F., 2017. OsARM1, an R2R3 MYB transcription factor, is involved in regulation of the response to arsenic stress in rice. *Front. Plant Sci.* 8. <https://doi.org/10.3389/fpls.2017.01868>.
- Wang, J., Qi, M., Liu, J., Zhang, Y., 2015. CARMO: a comprehensive annotation platform for functional exploration of rice multi-omics data. *Plant J.* 83, 359–374. <https://doi.org/10.1111/tpj.12894>.
- Wang, L., Ying, Y., Narsai, R., Ye, L., Zheng, L., Tian, J., Whelan, J., Shou, H., 2013. Identification of OsBHLH133 as a regulator of iron distribution between roots and shoots in *Oryza sativa*. *Plant Cell Environ.* 36, 224–236. <https://doi.org/10.1111/j.1365-3040.2012.02569.x>.
- Wang, S., Li, L., Ying, Y., Wang, J., Shao, J.F., Yamaji, N., Whelan, J., Ma, J.F., Shou, H., 2020. A transcription factor OsBHLH156 regulates Strategy II iron acquisition through localising IRO2 to the nucleus in rice. *New Phytol.* 225, 1247–1260. <https://doi.org/10.1111/nph.16232>.
- Waters, B.M., Armbrust, L.C., 2013. Optimal copper supply is required for normal plant iron deficiency responses. *Plant Signal. Behav.* 8, e26611. <https://doi.org/10.4161/psb.26611>.
- Waters, B.M., McInturf, S.A., Stein, R.J., 2012. Rosette iron deficiency transcript and microRNA profiling reveals links between copper and iron homeostasis in *Arabidopsis thaliana*. *J. Exp. Bot.* 63, 5903–5918. <https://doi.org/10.1093/jxb/ers239>.
- Wu, Q., Liu, C., Wang, Z., Gao, T., Liu, Y., Xia, Y., Yin, R., Qi, M., 2022. Zinc regulation of iron uptake and translocation in rice (*Oryza sativa* L.): implication from stable iron isotopes and transporter genes. *Environ. Pollut.* 297, 118818. <https://doi.org/10.1016/j.envpol.2022.118818>.
- Yacoubi, I., Gadaleta, A., Mathlouthi, N., Hamdi, K., Giancaspro, A., 2022. Abscisic acid-stress-ripening genes involved in plant response to high salinity and water deficit in durum and common wheat. *Front. Plant Sci.* 13. <https://doi.org/10.3389/fpls.2022.789701>.
- Yan, L., Riaz, M., Liu, J., Yu, M., Cuncang, J., 2022. The aluminum tolerance and detoxification mechanisms in plants; recent advances and prospects. *Crit. Rev. Environ. Sci. Technol.* 52, 1491–1527. <https://doi.org/10.1080/10643389.2020.1859306>.
- Yang, J., Fan, W., Zheng, S., 2019. Mechanisms and regulation of aluminum-induced secretion of organic acid anions from plant roots. *J. Zhejiang Univ. - Sci. B* 20, 513–527. <https://doi.org/10.1631/jzus.B1900188>.
- Yang, X., Liu, C., Liang, C., Wang, T., Tian, J., 2024. The phosphorus-iron nexus: decoding the nutrients interaction in soil and plant. *Int. J. Mol. Sci.* 25, 6992. <https://doi.org/10.3390/ijms25136992>.
- Zhang, C., Shinwari, K., Luo, L., Zheng, L., 2018. OsYSL13 is involved in iron distribution in rice. *Int. J. Mol. Sci.* 19, 3537. <https://doi.org/10.3390/ijms19113537>.
- Zhang, M., Pinson, S.R.M., Tarpley, L., Huang, X.-Y., Lahner, B., Yakubova, E., Baxter, I., Guerinot, M. Lou, Salt, D.E., 2014. Mapping and validation of quantitative trait loci associated with concentrations of 16 elements in unmilled rice grain. *Theor. Appl. Genet.* 127, 137–165. <https://doi.org/10.1007/s00122-013-2207-5>.
- Zhang, P., Zhong, K., Zhong, Z., Tong, H., 2019. Mining candidate gene for rice aluminum tolerance through genome wide association study and transcriptomic analysis. *BMC Plant Biol.* 19, 490. <https://doi.org/10.1186/s12870-019-2036-z>.
- Zhang, W., Guan, M., Chen, M., Lin, X., Xu, P., Cao, Z., 2024. Mutation of OsNRAMP5 reduces cadmium xylem and phloem transport in rice plants and its physiological mechanism. *Environ. Pollut.* 341, 122928. <https://doi.org/10.1016/j.envpol.2023.122928>.
- Zhao, H., Frank, T., Tan, Y., Zhou, C., Jabnoute, M., Arpat, A.B., Cui, H., Huang, J., He, Z., Poirier, Y., Engel, K., Shu, Q., 2016. Disruption of OsSULT3;3 reduces phytate and phosphorus concentrations and alters the metabolite profile in rice grains. *New Phytol.* 211, 926–939. <https://doi.org/10.1111/nph.13969>.
- Zheng, Luqing, Ying, Y., Wang, L., Wang, F., Whelan, J., Shou, H., 2010. Identification of a novel iron regulated basic helix-loop-helix protein involved in Fe homeostasis in *Oryza sativa*. *BMC Plant Biol.* 10, 166. <https://doi.org/10.1186/1471-2229-10-166>.